Enzyme Activity Profiles during Fruit Development in Tomato Cultivars and *Solanum pennellii*[1][W][OA]

Marie-Caroline Steinhauser*, Dirk Steinhauser, Karin Koehl, Fernando Carrari, Yves Gibon[2], Alisdair R. Fernie, and Mark Stitt

Max Planck Institute of Molecular Plant Physiology, 14476 Potsdam-Golm, Germany (M.-C.S., D.S., K.K., Y.G., A.R.F., M.S.); and Instituto de Biotecnología, Centro de Investigación en Ciencias Veterinarias y Agronómicas, Instituto Nacional de Tecnología Agropecuaria, B1712WAA Castelar, Argentina (F.C.)

Enzymes interact to generate metabolic networks. The activities of more than 22 enzymes from central metabolism were profiled during the development of fruit of the modern tomato cultivar *Solanum lycopersicum* 'M82' and its wild relative *Solanum pennellii* (LA0716). In *S. pennellii*, the mature fruit remains green and contains lower sugar and higher organic acid levels. These genotypes are the parents of a widely used near introgression line population. Enzymes were also profiled in a second cultivar, *S. lycopersicum* 'Moneymaker', for which data sets for the developmental changes of metabolites and transcripts are available. Whereas most enzyme activities declined during fruit development in the modern *S. lycopersicum* cultivars, they remained high or even increased in *S. pennellii*, especially enzymes required for organic acid synthesis. The enzyme profiles were sufficiently characteristic to allow stages of development and cultivars and the wild species to be distinguished by principal component analysis and clustering. Many enzymes showed coordinated changes during fruit development of a given genotype. Comparison of the correlation matrices revealed a large overlap between the two modern cultivars and considerable overlap with *S. pennellii*, indicating that despite the very different development responses, some basic modules are retained. Comparison of enzyme activity, metabolite profiles, and transcript profiles in *S. lycopersicum* 'Moneymaker' revealed remarkably little connectivity between the developmental changes of transcripts and enzymes and even less between enzymes and metabolites. We discuss the concept that the metabolite profile is an emergent property that is generated by complex network interactions.

The cultivated tomato, *Solanum lycopersicum*, is the second most important noncereal crop worldwide and an important model species for fruit physiology and development, quantitative genetics, and plant breeding (Tanksley et al., 1995; Giovannoni, 2001; Zamir, 2001; Mueller et al., 2005a; Lippman et al., 2007). It has been used to study fruit shape and development (Causse et al., 2004; Brewer et al., 2007; Bertin et al., 2009), metabolite composition (Fridman et al., 2004; Tikunov et al., 2005; Schauer et al., 2006; Tieman et al., 2006; Bertin et al., 2009), flowering time (Jimenez-Gomez et al., 2007), disease and fungus resistance (Chaerani et al., 2007; Finkers et al., 2007), tolerance to salinity (Cuartero et al., 2006; Villalta et al., 2007), and chilling (John Goodstal et al., 2005).

The cultivated tomato has limited genetic variability, due to natural and artificial selections that occurred during domestication and evolution of modern cultivars (Rick, 1976). However, there are very large genetic resources available for research, including modern inbreds, saturated mutagenesis populations that support TILLING (Menda et al., 2004; Till et al., 2006), a phenotyped core collection of 7,000 accessions representing heirloom varieties, ancient varieties, and wild species, and several inbred lines that have been generated by crossing *S. lycopersicum* with wild relatives from the so-called "*esculentum* complex" (Knapp et al., 2004). The wild species are an especially rich source of desirable genetic diversity. In particular, a set of 76 near isogenic lines derived from an *S. lycopersicum* 'M82' × *Solanum pennellii* cross (Eshed and Zamir, 1994) has been subjected to extensive agronomic, physiological, and molecular phenotyping (Lippman et al., 2007). This has allowed quantitative trait loci (QTLs) to be detected that affect morphology and yield (Semel et al., 2006), fruit coloration (Liu et al., 2003), metabolite levels (Causse et al., 2004; Fridman et al., 2004; Baxter et al., 2005a; Schauer et al., 2006), volatile metabolites (Tieman et al., 2006), and antioxidants (Rousseaux et al., 2005). The cultivated tomato is one of the first examples of a crop plant that has benefited

significantly from exotic germplasm introgression (Zamir, 2001; Lippman et al., 2007).

An expanding range of molecular and genomics tools are available for tomato, including facile transformation (Klee et al., 1991), a large EST collection (Van der Hoeven et al., 2002), oligonucleotide-based arrays (Slocombe et al., 2008; Wang et al., 2009), emerging genome sequence information (Mueller et al., 2005a, 2005b), and a wide range of phenotyping (Causse et al., 2004) and metabolite profiling (Tikunov et al., 2005; Schauer et al., 2006; Fraser et al., 2007) technologies. Very recently, a prepublication tomato genome sequence was made available by the International Tomato Genome Sequencing Consortium (http:// solgenomics.net/). Expression profiling has been used to study transcriptomic changes of six introgression lines along a developmental series (Baxter et al., 2005b). Metabolite profiling has been applied to analyze changes during fruit development (Carrari et al., 2006), to phenotype inbred lines, and to identify large numbers of metabolite QTLs (Schauer et al., 2006). Networks obtained by combining transcript and metabolite profiles have been used to explore metabolic programs that underlie tomato fruit development (Carrari and Fernie, 2006) and to short-list genes that may regulate fruit composition (Mounet et al., 2009).

However, as in other model systems, there is relatively little information available about changes of proteins and enzyme activities in tomato fruit. This is at least partly for technical reasons. While custom-made or commercial arrays are available for transcript profiling and widely used techniques like gas chromatography-mass spectrometry and liquid chromatography-mass spectrometry are available for metabolite profiling, it is still a technical challenge to obtain quantitative information about large numbers of proteins (Rose et al., 2004; Baerenfaller et al., 2008) or enzyme activities (Mitchell-Olds and Pedersen, 1998; Prioul et al., 1999; Thevenot et al., 2005; Cross et al., 2006). While there have been many studies of the developmental changes of small sets of enzymes in tomato fruits (Robinson et al., 1988; Yelle et al., 1988), medium-size surveys are limited to a study of 13 enzymes during fruit development in *S. lycopersicum* 'MicroTom' (Obiadalla-Ali et al., 2004). The availability of wild relatives provides a resource to deepen our understanding of the regulation of central metabolism during tomato fruit development. Kortstee et al. (2007) investigated the responses of nine enzymes in *S. lycopersicum* 'Moneymaker' ('MM') and two wild relatives (*Solanum peruvianum* and *Solanum habrochaites*) of tomato. However, this study was restricted to the first stages of fruit development, where the changes in metabolism during fruit ripening are qualitatively similar to those in *S. lycopersicum* and result in even higher levels of soluble sugars.

Recently, Faurobert et al. (2007) pioneered the large-scale use of proteomics to document abundance changes of 90 proteins during fruit development in a cherry tomato cultivar, including 15 proteins associated with carbohydrate metabolism, five with photosynthesis and respiration, nine with amino acid metabolism, five with secondary metabolism, and one each for vitamin and lipid metabolism. Proteins involved in amino acid and protein synthesis were most abundant in very young fruit, proteins for photosynthesis and cell wall expansion increased transiently during the expansion phase, and proteins related to carbon metabolism and stress rose later in development. However, analogous approaches have not yet been applied to wild relatives of tomato.

We recently established robotized activity assays for over 20 enzymes from central metabolism in Arabidopsis (*Arabidopsis thaliana*) leaves (Gibon et al., 2004; Sulpice et al., 2007). This platform has been used to investigate the response of these enzymes to diurnal cycles, to the carbon and nutrient status, and to temperature (Gibon et al., 2004, 2006; Morcuende et al., 2007; Osuna et al., 2007; Usadel et al., 2008) and to map enzyme activity QTLs in a Cape Verde Islands × Landsberg *erecta* Arabidopsis recombinant inbred line population (Keurentjes et al., 2008). Here, we adapt the existing enzyme-profiling platform to measure a large set of enzymes in primary metabolism. This platform is used to compare the changes of enzyme activity during fruit development in *S. lycopersicum* 'M82' and *S. pennellii*. The latter is a wild relative with a markedly different fruit development process in which the mature fruit remains green and contains lower sugar and higher organic acid levels than modern cultivars (Schauer et al., 2006). Our main aim was to compare the developmental changes of enzyme activities that underlie the differing metabolite profiles in these two contrasting genotypes, which are the crossing parents for a widely used near isogenic line population (see above). In addition, we have profiled enzyme activities in a second cultivar, *S. lycopersicum* 'MM'. This was done to provide a comparison with *S. lycopersicum* 'M82' and to allow the developmental changes of enzyme activities to be compared with large data sets that are already available for the developmental changes of metabolites and transcripts in *S. lycopersicum* 'MM' (Carrari et al., 2006).

RESULTS

Optimization of Sample Handling and Enzyme Assays

The enzymes measured by the platform, their abbreviations, and assay principles are listed in Supplemental Tables S1 and S2; their EC numbers, catalyzed reactions, and sites in metabolism are summarized in Supplemental Figure S1. Standard sample handling involved freezing of tomato fruit pericarp in liquid N_2, storage at $-80°C$, homogenization in liquid N_2, subaliquoting into small weighted aliquots at low temperature, extraction by vigorous shaking in extraction buffer, snap freezing, rethawing, and robotized aliquoting into flat-bottom microtiter plates, which al-

ready contained the assay mix. Activities were mainly measured using stopped assays. The inactivated assay mix was stored at −20°C until the next day and neutralized, and the product was determined, usually in a sensitive enzymatic cycling reaction (compare with Supplemental Fig. S2). This allows activities to be measured at very high dilutions (Gibon et al., 2004) and decreases interference from other components in the extract.

Many enzyme activities are lower in tomato fruits than Arabidopsis leaves. Sample handling and assays, therefore, were reoptimized, as depicted in Supplemental Figure S3, with fructokinase (FruK) as an example. For routine measurements, extraction was performed with a modified buffer with higher glycerol and Triton X-100 concentrations. Some enzymes showed higher and none showed lower activities (data not shown) compared with the buffer used by Gibon et al. (2004). To allow accurate weighing, the standard extraction procedure used about 20 mg fresh weight. The optimal dilution ratio for tomato fruit material was between 1 mg fresh weight of tomato fruit per 0.45 and 1.5 mL of assay mix for most enzymes (Supplemental Table S2; Supplemental Fig. S3A). As all enzyme reactions were linear for at least 70 min (Supplemental Fig. S3B; data not shown), the duration of the stopped assays was standardized as 60 min (compare with Supplemental Fig. S3B). As two enzymes, FruK (Supplemental Fig. S3C) and NADP-dependent isocitrate dehydrogenase (NADP-IcDH), showed loss of activity during a freeze-thaw cycle, we routinely assayed all enzymes immediately after extract preparation. All dilution and assay steps were performed using a pipetting robot. This enabled the measurement of 28 enzyme activities in 80 samples in 2 d. To check that there was no loss of activity of enzymes due to inhibitory components in the tomato fruit extracts, spike-in studies were performed in which powdered Arabidopsis leaf and tomato pericarp were extracted and assayed on their own or were mixed 1:1 before extraction and assayed. Recoveries lay between 67% and 106% of the expected values (compare with Supplemental Fig. S3D; data not shown).

Fruit Development in *S. lycopersicum* 'M82', *S. lycopersicum* 'MM', and *S. pennellii*

Under the established growth conditions, fruit ripening in *S. lycopersicum* cultivars occurs over a period of approximately 70 d after anthesis (DAA; Carrari et al., 2006). Fruit development in *S. lycopersicum* can be visually monitored by the external index (Fig. 1A), which allows fruit development to be divided into four main phases (Gillaspy et al., 1993): I, cell differentiation; II, cell division, corresponding to small green fruits harvested from 7 to 21 DAA; III, cell expansion, corresponding to between 28 DAA and the first visible carotenoid accumulation (i.e. the breaker stage) at around 45 and 56 DAA in M82 and MM, respectively; and IV, fruit ripening, between 49 to 70

DAA and 63 to 70 DAA for M82 and MM, respectively. Fruits of the wild relative *S. pennellii* ripen between 70 and 80 d after pollination, on or off the vine (Grumet et al., 1981). Ripening is characterized by fruit softening, which can lead to split opening of the fruits upon slight pressure. However, there are no obvious visual indicators for ripening stages (Fig. 1B). Therefore, it was necessary to develop methods to assess the developmental stage.

To allow nondestructive monitoring of fruit size, height (i.e. the length from the peduncle attachment to the base of the fruit) and diameter were measured and used to calculate the fruit volume: $V = 4/3\pi abc$, where a, b, and c correspond to the three elliptic radii, with radius a being half the length and b and c being identical and equal to the half-width of the fruit. In a preliminary experiment, these parameters were measured and used to calculate the volume before harvesting and weighing the fruit. The estimated volume and weight of the fruit were very similar in *S. lycopersicum* 'M82' (Fig. 1C) and *S. pennellii* (Fig. 1D; $r = 0.983$ and 0.961, respectively; $P < 1e{-}10$).

To investigate the time dependence of fruit growth in *S. lycopersicum*, individual flowers were tagged at anthesis. The size of *S. lycopersicum* 'M82' fruit increased in a sigmoidal manner with time, reaching a final size (35 ± 10 cm^2) at about 42 DAA, corresponding to the breaker stage (Fig. 1A). There was no further increase in size during ripening (Fig. 1E). A similar response was seen for *S. lycopersicum* 'MM' (data not shown), except that the fruits were larger and breaker stage was not reached until about 56 DAA (Carrari et al., 2006). Tagging of individual flowers was not possible for *S. pennellii*, because the peduncle broke under slight pressure. Instead, DAA was estimated for each fruit from time-lapse photographs (Fig. 1F). *S. pennellii* fruits grew continuously until 70 DAA. The final size (2.0 ± 0.5 cm^2) was much smaller than for *S. lycopersicum* cultivars. Fully ripe green fruits were obtained at about 70 DAA, as reported previously (see above). These ripe fruits were soft, and some exploded or fell off due to peduncle breakage (data not shown). Only fruits that ripened on the vine and did not split were harvested for enzymatic analyses.

Developmental Changes of Enzyme Activities in *S. lycopersicum* 'M82', *S. lycopersicum* 'MM', and *S. pennellii*

Enzyme activities were measured in fruits harvested at 28, 35, 42, 49, 56, 63, and 70 DAA for the three genotypes. Many of the following analyses exclude 28 and 70 DAA, because fewer samples were collected at these stages. The results for DAA 35 to 63 are summarized in Figure 2 (for the original data, see Supplemental Tables S3–S5). While each enzyme has a similar activity range, the developmental changes differ between genotypes. This is especially so for the comparison between the two *S. lycopersicum* cultivars and the wild relative *S. pennellii*.
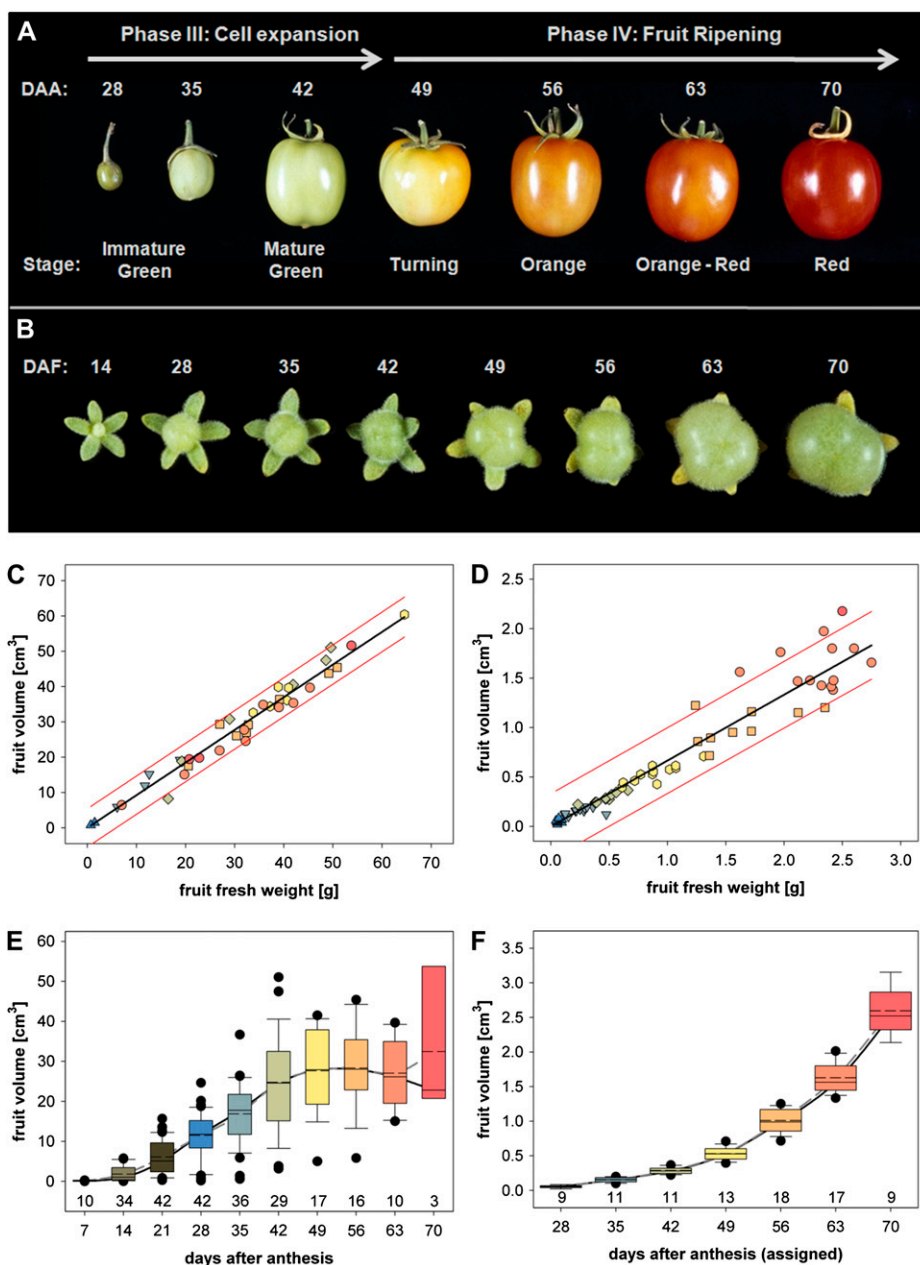
Figure 1. A and B, Growth characteristics of fruits harvested at different time points during development of the red-fruited *S. lycopersicum* 'M82' (A) and the green-fruited *S. pennellii* (B). The DAA and DAF are depicted. The phases and stages of fruit development of *S. lycopersicum* 'M82' are assigned according to Gillaspy et al. (1993). C and D, Scatterplots and regression plots of the fruit fresh weight (g) and the fruit volume (cm³) of the red-fruited *S. lycopersicum* 'M82' (C) and the green-fruited *S. pennellii* (D). The black solid lines represent the regression line of a linear fit according to $y = mx$ with the slope m. The red lines indicate the 95% confidence band, a measure of certainty. The colors and symbols used in each plot indicate the monitored or assigned DAA (for details, see below): 28 = dark blue triangle (up), 35 = light blue triangle (down), 42 = light green diamond, 49 = yellow hexagon, 56 = orange square, 63 = light red circle, and 70 = dark red circle. E and F, Boxplot graphs illustrating the changes in fruit volume during the development of the red-fruited *S. lycopersicum* 'M82' (E) and the green-fruited *S. pennellii* (F). Flowers of *S. lycopersicum* 'M82' and *S. pennellii* from two independent experiments growing under greenhouse conditions were tagged, and fruits were harvested at the indicated time points after anthesis (DAA). Fruit height and diameter were measured to calculate the fruit volume (cm³). The number of samples used is indicated at the bottom of each graph. The median and the mean are indicated by solid and dashed lines in each box, respectively. To aid interpretation, the median and the mean values of each DAA are connected by a black solid line and a gray dashed line, respectively. Outlier values are depicted by solid black circles.
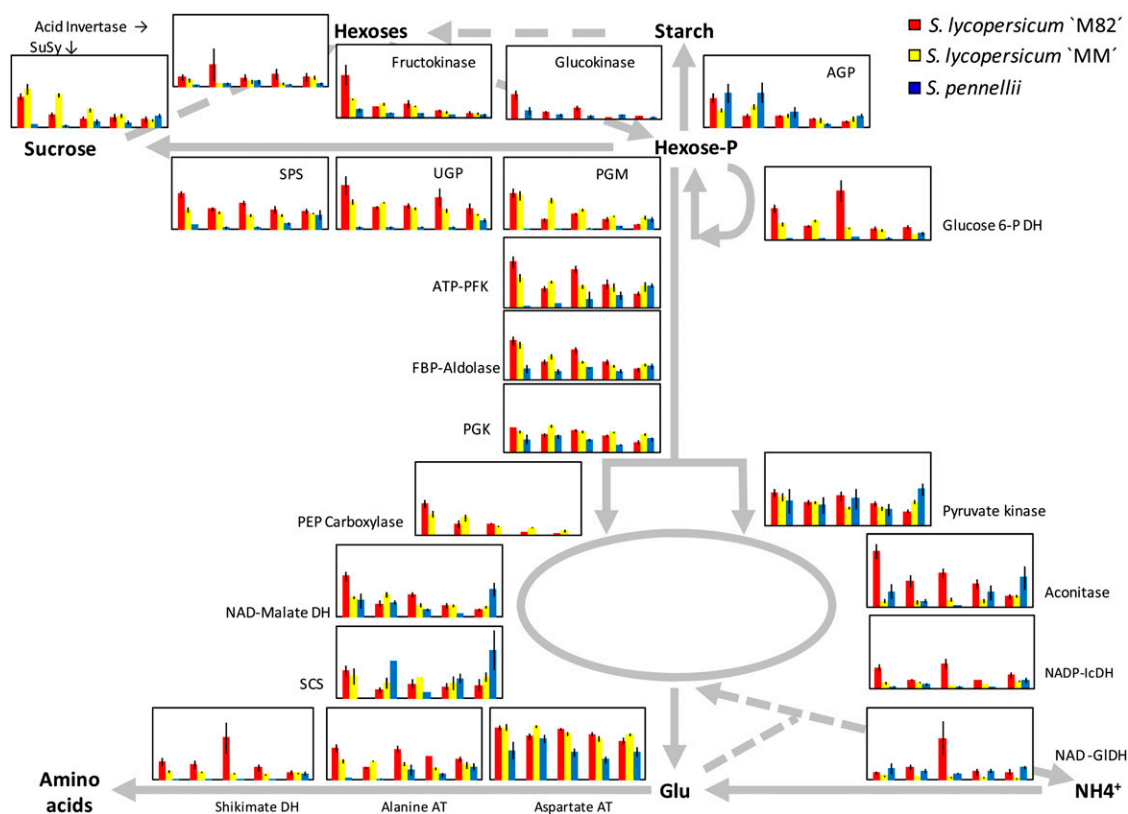
Figure 2. Overview of the enzyme activities mapped onto metabolic pathways in the red-fruited *S. lycopersicum* 'M82' (red bars), *S. lycopersicum* 'MM' (yellow bars), and the green-fruited *S. pennellii* (blue bars). Enzyme activities (expressed as nmol g^{-1} fresh weight min^{-1}; compare with Supplemental Tables S3–S5) for the majority of the 28 determined enzymes are depicted as bar diagrams including SE bars according to the DAA group, namely 35, 42, 49, 56, and 63 DAA (left to right). The very early (28 DAA) and the very late (70 DAA) stages are not visualized and statistically assessed due to few measurements being available at these time points for *S. lycopersicum* 'M82'. The growth and harvest of *S. lycopersicum* 'M82' and *S. pennellii* were performed at the same season and time, whereas *S. lycopersicum* 'MM' was grown separately. The data, including statistical assessments, are available in Supplemental Tables S3 to S5.

In *S. lycopersicum* 'M82', most enzymes have a high activity in the youngest stage, and activity decreases during expansion and ripening. There was an especially large decrease of the activities of enzymes involved in Suc degradation (including Suc synthase [SuSy], FruK, glucokinase [GlcK]), starch synthesis (ADP-Glc pyrophosphorylase [AGP]), and organic acid synthesis (phospho*enol*pyruvate carboxylase [PEPC], NAD-dependent malate dehydrogenase [NAD-MDH]). There was a smaller 2- to 3-fold decrease of the activities of enzymes required for Suc synthesis (Suc-P synthase [SPS], UDP-Glc pyrophosphorylase [UGP]), glycolysis (ATP-dependent phosphofructokinase [ATP-PFK], aldolase, phosphoglycerokinase [PGK], pyruvate kinase), and several enzymes from the tricarboxylic acid cycle (aconitase, NADP-IcDH, succinyl-CoA ligase). Enzymes involved in nitrogen metabolism remain relatively high throughout development (Ala aminotransferase [AlaAT], Asp aminotransferase [AspAT], NAD-dependent Glu dehydrogenase [NAD-GlDH], shikimate dehydrogenase [ShkDH]). Several enzymes show relatively high activity at 49 DAA, correspond-

ing to the turning or "breaker" stage. Acid invertase activity changed independently of the other enzymes.

S. lycopersicum 'MM' also showed a decrease in the activity of most enzymes during fruit development. Compared with *S. lycopersicum* 'M82', several enzyme activities were lower at the first harvest point at 35 DAA (aconitase, AGP, FruK, NAD-dependent glyceraldehyde-3-phosphate dehydrogenase [NAD-GAPDH], NADP-dependent GAPDH [NADP-GAPDH], NAD-MDH, PEPC, pyruvate kinase), and the transient peak at 49 DAA was absent or less marked. A weak peak or shoulder was often discernible at 42 DAA (AlaAT, aldolase, AspAT, ATP-PFK, FruK, Glc-6-P dehydrogenase [G6PDH], NAD-GlDH, NAD-MDH, PEPC, phosphoglucose isomerase (PGI), phosphoglucose mutase (PGM), pyruvate kinase, ShkDH, SPS).

S. pennellii showed a markedly different developmental pattern. AGP activity was initially high and decreased during fruit development. Most enzymes from glycolysis and the tricarboxylic acid cycle showed rather stable activities, with a decline in mid development and an increase at later stages. Several

enzymes involved in Suc synthesis (SPS, UGP, PGM), Suc breakdown (SuSy), and amino acid metabolism (ShkDH, AlaAT, NAD-GlDH) were low in young fruit and rose during fruit ripening. Invertase activity changed independently of the other enzymes, as already seen for the two *S. lycopersicum* cultivars. At 63 DAA, the activities of most enzymes in *S. pennellii* are comparable to or higher than in *S. lycopersicum* (compare with Fig. 2).

The data set was next subjected to a series of statistical analyses to investigate whether enzyme activity profiles can be used to distinguish between developmental stages and genotypes and to investigate and compare correlation networks in the three genotypes. As the complete data set contained some missing values, samples or enzyme activities with a high number of missing values were removed, and box plots were used to identify and remove outliers (see "Materials and Methods"), resulting in three separate shrunk and outlier-removed data sets for each genotype. They contain data for 27 enzymes for *S. lycopersicum* 'M82', 25 enzymes in *S. lycopersicum* 'MM', and 25 enzymes in *S. pennellii*. Validated replicated measurements were available for all three genotypes for 22 enzymes. The latter were normalized for each genotype and fused to generate a combined shrunk data set containing data for the same 22 enzymes for all three genotypes. An overview of the shrunk data sets is provided in Supplemental Table S6.

Clustering of Enzyme Activities in *S. lycopersicum* 'M82', *S. lycopersicum* 'MM', and *S. pennellii*

We first investigated whether the developmental changes of enzyme activities allow the fruit samples to be clustered into groups that reflect the fruit developmental stage. Clustering was performed separately for each genotype, using 27 enzymes for *S. lycopersicum* 'M82', 25 for *S. lycopersicum* 'MM', and 25 for *S. pennellii* (Supplemental Fig. S4). While visual inspection revealed some coclustering of samples according to fruit age at harvest, this was partly masked by the arbitrary order of samples within the individual branches. The cluster trees, therefore, were manually cut at the positions indicated in Supplemental Figure S4. This generated three main clusters and an outlier group for each genotype (Table I).

For *S. lycopersicum* 'M82', the vast majority of the samples from young fruit (35 DAA) were found in one cluster, those from mid development fruit (42–49 DAA) were found in a second cluster, and those from ripening fruit (56–70 DAA) were found in a third cluster. A similar distribution was found for *S. lycopersicum* 'MM' (except that the age classes are 28 DAA, 35–49 DAA, and 56–70 DAA) and *S. pennellii* (except that the age classes are 28–42 DAA, 49–56 DAA, and 63–70 DAA). In all cases, the outlier group contains samples from DAA 63 to 70. Thus, in all three genotypes, three overall groups can be defined: (1) samples harvested in early "growth"-related stages; (2) sam-

ples harvested during the transition from growth to early ripening; and (3) samples harvested later in the ripening process.

The validity of clusters in Table I was checked by applying a bootstrap strategy to the three underlying shrunk matrices followed by consensus tree building (see "Materials and Methods"). The clusters derived from the consensus trees (data not shown) were very similar or identical to the clusters in Table I. Moreover, a strong Pearson matrix correlation based on Mantel test was found between the nonaveraged and the averaged bootstrapped matrices ($r > 0.98$, $P < 1e-04$).

Principal Component Analysis of Enzyme Activities in *S. lycopersicum* 'M82', *S. lycopersicum* 'MM', and *S. pennellii*

We used principal component analysis to investigate whether the three genotypes can be statistically distinguished by the enzyme activity profiles at the various developmental stages (Fig. 3). This cross-genotype analysis was performed with the combined shrunk data set for 22 enzymes.

The samples from the two *S. lycopersicum* cultivars were superimposed on each other. The first and second components separated them according to their developmental state, with samples from young fruits grouping at the upper left hand side and mature fruits in the lower right hand side, with a similar trajectory for both cultivars (Fig. 3A). The early stage samples from *S. lycopersicum* 'MM' were slightly farther to the right and lower on the trajectory to mature fruit than the early stage samples from *S. lycopersicum* 'M82', which is consistent with the former maturing slightly later.

S. pennellii showed a completely different response. The immature fruit samples grouped close to partially mature fruits of the commercial cultivars, and mature fruits were clearly separated from the modern cultivars.

The loadings of the enzymes in the first two principal components are shown in Figure 3B. The separation of developmental stages in the modern cultivars and their separation from *S. pennellii* are driven by a large number of enzymes, including invertase, pyrophosphate:Fru-6-P 1-phosphotransferase (PPi-PFK), PGM, G6PDH, AGP, and NAD-GAPDH and, to a lesser extent, AlaAT, ShkDH, UGP, aconitase, NAD-MDH, aldolase, and FruK.

Network Analysis of Enzyme Activities in *S. lycopersicum* 'M82', *S. lycopersicum* 'MM', and *S. pennellii*

We next investigated the correlation networks that are generated by computing pairwise correlations between enzymes in the developmental series for each genotype (Supplemental Fig. S5). Although the analysis was performed separately for each genotype, to allow comparison between genotypes we used the shrunk data set of 22 enzymes for which complete data

Table I. *Overview of clusters obtained from average linkage clustering on Euclidean distances among the DAA groups for the different cultivars and species under investigation*

The original cluster tree and the manual cut clusters are shown in Supplemental Figure S3. Cluster assignment to three main groups and one outlier group was done manually. The number and frequency (in parentheses) are given for each cluster and DAA group. Outlier groups are specified at the bottom. Significant enrichments ($P < 0.05$), tested with Fisher's exact test, for each cluster and DAA group are indicated in boldface. Samples with only one replicate were removed and are depicted in italics. Asterisks represent potential developmental groups manually assigned according to the results obtained from enrichment analyses in conjunction with the underlying sample frequency.

Species:	S. lycopersicum 'M82'			S. lycopersicum 'MM'			S. pennellii		
Cluster:	I	II	III	I	II	III	I (a + b)	II	III
Size:	9	15	18	6	16	19	17	14	16
28 DAA	*	*1 (100)*		**5 (83.3)***	1 (16.7)		**5 (100)***		
35 DAA	**7 (77.8)***	2 (22.2)		1 (16.7)	**4 (66.7)***	1 (16.7)	**3 (60)***	2 (40)	
42 DAA	1 (11.1)	**3 (33.3)***	5 (55.6)		**6 (100)***		**5 (62.5)***	3 (37.5)	
49 DAA	1 (14.3)	**6 (85.7)***			**4 (66.7)***	2 (33.3)	2 (33.3)	**2 (33.3)***	2 (33.3)
56 DAA		3 (33.3)	**6 (66.7)***			**6 (100)***	1 (10)	**6 (60)***	3 (30)
63 DAA			**6 (75)***		1 (16.7)	**4 (66.7)***	1 (12.5)	1 (12.5)	**5 (62.5)***
70 DAA			*1 (100)**			**6 (100)***			**6 (85.7)***
Outlier groups	63J, 63G			63A			63D, 70C		

sets were available for all three genotypes. Key features of the correlation analysis are summarized in Table II and Figure 4. There are a large number of correlations between enzymes in *S. lycopersicum* 'M82' and *S. lycopersicum* 'MM' and a somewhat smaller number of correlations in *S. pennellii* (compare with Supplemental Fig. S5).

Of a total of 231 possible pairwise connections, 151 and 190 were significant ($P_{adj} < 0.05$) in *S. lycopersicum* 'M82' and *S. lycopersicum* 'MM', respectively. Strikingly, at this significance level, almost all of the correlations are positive (Table II). A majority (120) of the pairwise correlations were shared between these two genotypes (Fig. 4), emphasizing the strong similarity between the networks in the two cultivars. In *S. lycopersicum* 'M82', the highly connected enzymes (more than 11 out of 22 possible connections) included AlaAT, AspAT, aldolase,

G6PDH, ATP-PFK, NAD-GAPDH, PGK, pyruvate kinase (PK), PPi-PFK, PGI, PGM, SuSy, AGP, SPS, aconitase, NAD-MDH, and NADP-IcDH (Table II). These enzymes were all equally or even more tightly connected in *S. lycopersicum* 'MM', except for aconitase. Some enzymes that were relatively well connected in *S. lycopersicum* 'M82' became tightly connected in *S. lycopersicum* 'MM' (e.g. G6PDH, PK, SuSy), and some enzymes that were poorly connected in *S. lycopersicum* 'M82' became tightly connected in *S. lycopersicum* 'MM' (NAD-GlDH, ShkDH, FruK, UGP; Table II).

There were fewer pairwise correlations (106) between enzymes in *S. pennellii* (Fig. 4). Individual enzymes with a large number of correlations in *S. pennellii* included AlaAT, ShkDH, PPi-PFK, NADP-IcDH, and UGP and, to a lesser extent, NAD-GlDH, G6PDH, NAD-GAPDH, PGK, AGP, aconitase, and
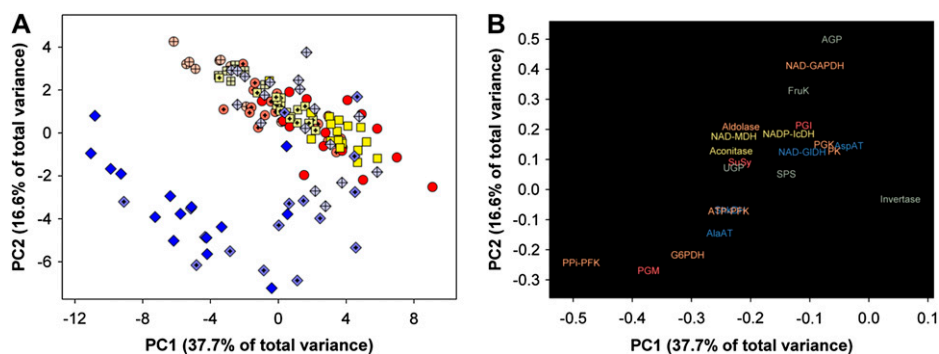

Figure 3. Principal component analysis of the shrunk data set comprising 22 enzyme activities in all three genotypes. A, Separation between the tomato cultivars and the wild relative for principal components 1 and 2. B, Contribution of enzymes for group separation. The genotypes depicted in A are color coded as follows: red circles = *S. lycopersicum* 'M82', yellow squares = *S. lycopersicum* 'MM', and blue diamonds = *S. pennellii*, with color shades according to early (bright color with crossed shape), mid (medium color with dotted shape), and late (dark color) groups of fruit development as determined by clustering and described in Table I. The enzymes depicted in B are color coded according to their functional/pathway assignment as follows: blue = amino acid metabolism, green = Suc and starch metabolism, light red = glycolysis, dark red = glycolysis and Suc and starch metabolism, and yellow = tricarboxylic acid cycle.

Table II. *Overview of the number of connections (degree centrality) found for significant positive and negative correlations in S. lycopersicum cultivars and S. pennellii*

The analyses were carried out separately in each genotype, using the shrunk data set with the same 22 enzymes in each genotype. To compute the degree centrality (i.e. the number of connections for each enzyme), the full correlation matrix (without the diagonal; i.e. each enzyme against itself) was converted into a network by considering only those associations that are statistically significant at $P_{adj} < 0.05$. An overlap matrix of all three genotypes can be found in Figure 5; a Venn diagram summarizing the shared correlations is depicted in Figure 4. Pathway abbreviations: AAM, amino acid metabolism; GGP, glycolysis/gluconeogenesis pathway; SSM, Suc and starch metabolism; TCA, tricarboxylic acid cycle.

Enzyme	Pathway	S. lycopersicum 'M82'		S. lycopersicum 'MM'		S. pennellii	
		Positive	Negative	Positive	Negative	Positive	Negative
AlaAT	AAM	12	0	18	1	15	0
AspAT	AAM	15	1	17	1	8	0
NAD-GlDH	AAM	2	5	17	0	9	0
ShkDH	AAM	2	4	20	0	13	0
Aldolase	GGP	17	0	16	0	7	0
G6PDH	GGP	13	0	20	1	9	0
ATP-PFK	GGP	16	1	19	0	8	0
NAD-GAPDH	GGP	18	0	18	1	10	1
PGK	GGP	16	1	14	0	10	0
PK	GGP	12	0	20	0	4	0
PPi-PFK	GGP	18	1	19	1	12	1
PGI	GGP|SSM	16	0	17	0	5	0
PGM	GGP|SSM	16	1	18	0	9	3
SuSy	GGP|SSM	13	1	19	1	6	0
AGP	SSM	15	0	20	1	9	2
FruK	SSM	10	0	18	0	6	1
Invertase	SSM	0	2	1	8	2	1
SPS	SSM	16	0	17	0	6	1
UGP	SSM	6	0	19	0	17	0
Aconitase	TCA	16	1	8	0	10	0
NAD-MDH	TCA	18	2	18	1	11	0
NADP-IcDH	TCA	15	0	11	0	16	0
Total (+/−)		282	20	364	16	202	10
Total		302		380		212	

NAD-MDH. Over one-half (63) and three-quarters (83) of the correlations in *S. pennellii* were shared with *S. lycopersicum* 'M82' and *S. lycopersicum* 'MM', respectively, and almost one-half (51) were shared with both modern cultivars.

This indicates that there is a core set of conserved correlations that is retained even though the developmental changes differ markedly between modern cultivars and the wild related species. Figure 5 depicts the 51 pairwise enzyme correlations that are shared across all three genotypes (shaded yellow) and the correlations that occur in only two (orange, red) or one (gray) of the genotypes. The enzymes showing the largest number of shared correlations across all three genotypes were AlaAT and PPi-PFK (10 and nine out of 21, respectively) followed by NAD-GAPDH (eight), NAD-MDH (seven), UGP, PGM, G6PDH, and AGP (six), ATP-PFK, PGK, aconitase, and NADP-IcDH (five), aldolase, SPS, AspAT, and FruK (four), SuSy (three), PGI (two), PK, NAD-GlDH, and ShkDH (one), and invertase (zero). The conserved features include many correlations between a set of enzymes in the upper part of glycolysis (UGP, PGM, ATP-PFK, PPi-PFK), correlations between enzymes in the lower part of glycolysis (NAD-GAPDH and to a lesser extent

PGK, AGP, AspAT), and correlations between AlaAT and a set of glycolytic enzymes (PGM, PGI, ATP-PFK, PPi-PFK, NAD-GAPDH, G6PDH, aconitase, NADP-IcDH). This highlights an integration of sectors of glycolysis with different sectors of nitrogen metabolism. Correlations that are present in both cultivars but absent in *S. pennellii* include a set of pairwise correlations between enzymes in the upper part of glycolysis (PGM, PGI, ATP-PFK, PPi-PFK, aldolase), enzymes in the lower part of glycolysis (NAD-GAPDH, PGK, PK), and enzymes in starch and Suc metabolism (SPS, SuSy, AGP). This may reflect differences in the metabolism of sugars, starch, and organic acids in the wild species. NAD-GlDH and invertase change in a rather independent manner than other enzymes in all three genotypes. The independent behavior of invertase is noteworthy, given that this enzyme may directly affect the accumulation of reducing sugars, which is an important metabolic trait in tomato fruit.

Changes of metabolite and transcript levels during fruit development have already been documented for *S. lycopersicum* 'MM' (Carrari et al., 2006). We used the same samples to analyze enzyme activities. This allowed us to fuse our *S. lycopersicum* 'MM' enzyme activity data set (Supplemental Table S4) with the
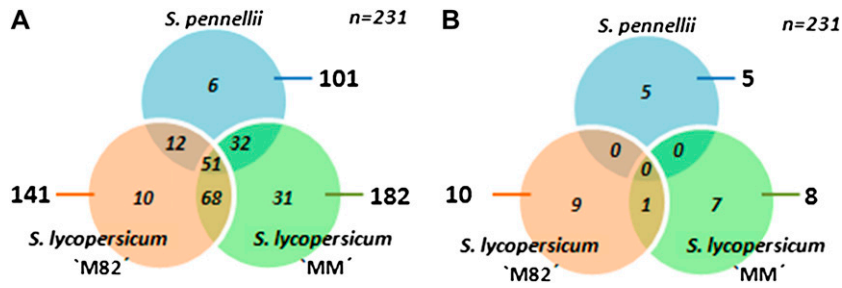
Figure 4. Venn diagrams of positive ($P_{adj} < 0.05$; A) and negative ($P_{adj} < 0.05$; B) significant correlations found in a genotype-specific data set and their overlaps for 22 enzymes reliably measured in all three genotypes. The numbers are extracted from the lower triangle (i.e. enzyme correlations between A versus B and B versus A were counted just once) without the diagonal (enzyme against itself) of the symmetric correlation matrix (Fig. 5). The number of enzymes is 22, and the number of all possible correlations is 231. The Venn diagrams show the total number of positive or negative significant correlations for each genotype-specific data set. The total number of significant correlations is shown outside the Venn sectors, the number of unique correlations of each genotype is shown in italics in the genotype-specific sector, and the number of shared significant correlations observed in two or all three data sets is depicted in italics in each of the overlaps.

metabolite (Fig. 6; Supplemental Table S7) and transcript data sets (Table III; Supplemental Table S8) and perform a joint correlation analysis. For this analysis, we used the shrunk and outlier-removed *S. lycopersicum* 'MM' data set for 25 enzymes.
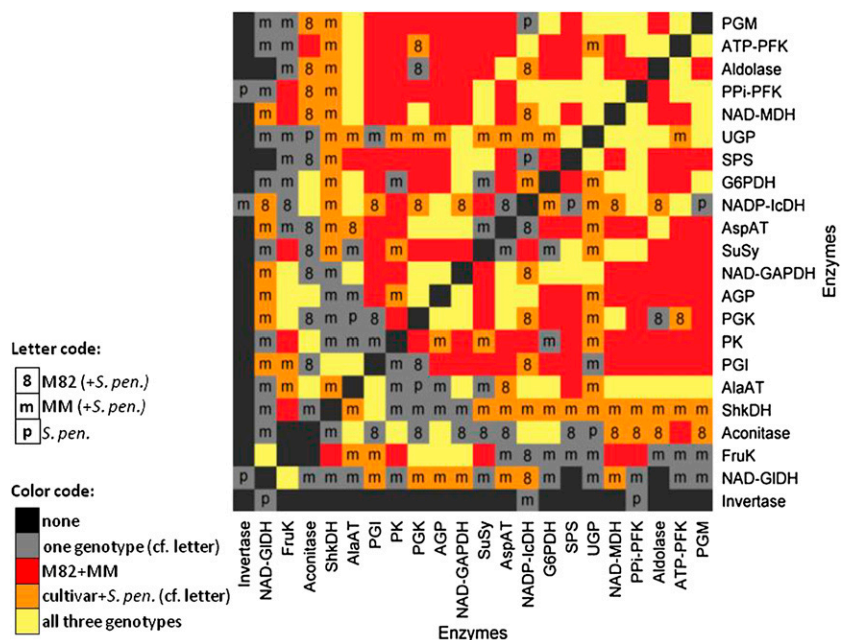
Comparison of Developmental Changes of Enzyme Activities and Metabolites in *S. lycopersicum* 'MM'

Figure 6 summarizes the correlation matrix between 25 enzymes and 85 metabolites during *S. lycopersicum* 'MM' fruit development. Enzymes are placed on the top and to the left, and metabolites are organized into structural classes (soluble sugars, sugar phosphates, tricarboxylic acid cycle intermediates, sugar alcohols, fatty acids, amino acids, cell wall components, organic acids, pigments) and placed on the bottom and to the right in the matrix. A more detailed display is provided in Supplemental Table S7.

As already noted (Figs. 4 and 5), many enzyme activities correlated with each other in *S. lycopersicum* 'MM' (231 out of 300 possible pairs in the shrunk, 25 enzyme activity MM-specific data set; $P_{adj} < 0.05$). The majority of these correlations were positive (see above). As previously discussed (Carrari et al., 2006), there were also many correlations between metabolites (in total, 740 [21%] and 327 [9%] of 3,570 possible pairs at $P < 0.05$ and $P < 0.01$, respectively; compare with Supplemental Table S7). In contrast to enzyme-enzyme pairs, 75% of the significant ($P < 0.05$) correlations between metabolites were positive and 25% were negative. Positive significant correlations were especially

Figure 5. Heat map of unique and overlapping significant pairwise enzyme activity correlations. The analysis is restricted to 22 enzymes for which complete data sets were available for all three genotypes, using a significance threshold of $P_{adj} < 0.05$. Enzymes that show a significant pairwise correlation in only one genotype are shaded gray, in both of the two cultivars are shaded red, between one cultivar and *S. pennellii* are shaded orange, and between all three genotypes are shaded yellow. The shading and the letter code for the significant pairwise correlation are depicted in the key within the heat map graph. The matrix diagonal (i.e. correlations of enzymes between themselves) and nonsignificant correlations are shaded dark gray. For counting the overlap among genotypes, only the half-matrix without the diagonal was considered (compare with Fig. 4), whereas the full symmetric correlation matrix is depicted here.
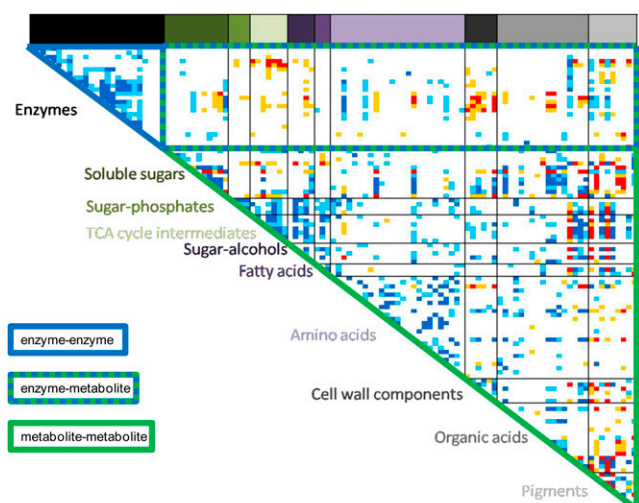
Figure 6. Heat map of the correlation matrix between enzymes and metabolites. The plot summarizes the Pearson correlation coefficients between enzyme activities (Supplemental Table S4) and metabolites (Carrari et al., 2006) in *S. lycopersicum* 'MM', measured in the samples from the same material. The parameters are grouped with enzyme activities in the left/top section and metabolites in the right/bottom section. Sectors corresponding to enzyme-enzyme, metabolite-metabolite, and enzyme-metabolite pairs are indicated. The color code for negative correlation is as follows: red if $P < -0.01$ and orange if $-0.01 < P < -0.05$; the color code for positive correlation is as follows: light blue if $0.01 < P < 0.05$ and dark blue if $P < 0.01$. The full data set is given in Supplemental Table S7.

frequent between related metabolites, including between soluble sugars (with the exception of Rha), between a set of metabolites that included intermediates from glycolysis and the tricarboxylic acid cycle, lipids, and sugar alcohols, between amino acids, between sugars isolated from the cell wall residue, and between metabolites involved in ascorbate metabolism. There were fewer correlations between enzyme activities and metabolites (in total, 219 [10%] and 55 [3%] of 2,125 possible pairs at $P < 0.05$ and $P < 0.01$, respectively). Of these, 41% were positive and 59% were negative at a significance threshold of $P < 0.05$.

The data set contained 28 enzyme-metabolite pairs where the metabolite was either the direct substrate or the direct product of the enzyme. No positive correlations were found between any enzyme and a metabolite that is its direct substrate or product. Two negative correlations were found between an enzyme activity and a substrate or product (AlaAT and α-ketoglutarate and AspAT and α-ketoglutarate [$P < 0.01$ and $P < 0.05$, respectively]; Supplemental Table S9). This indicates that the metabolite profile is mainly generated by an interaction between many enzymes rather than by changes of single enzymes. It is nevertheless interesting to see that these two aminotransferase activities are connected to α-ketoglutarate, which plays a key role in metabolism as a carbon acceptor during primary ammonium assimilation.

We also searched for correlations between individual enzymes and sets of metabolites that are located farther upstream or downstream in the pathway in which the enzyme is involved. ATP-PFK showed a very strong negative correlation with several tricarboxylic acid cycle intermediates, including citrate, aconitate, α-ketoglutarate, fumarate, malate, and (at a slightly relaxed P value of 0.07) isocitrate but not succinate. These correlations are unlikely to be due to a direct consequence of the changes in ATP-PFK activity; higher ATP-PFK activity would, on the simplest of assumptions, be expected to lead to an increase of glycolytic flux and an increase, rather than a decrease, in the levels of organic acids. ATP-PFK was also negatively correlated with glycerol-1-phosphate, shikimate, β-carotene, antheraxanthin, and zeaxanthin and positively correlated with Man. Again, there is no obvious simple casual explanation for these correlations. As a result of the network structure, many of these correlations are also found for other enzymes with which ATP-PFK was correlated, including AlaAT (malate, α-ketoglutarate, citrate, isocitrate, glycerol-1-phosphate, mannitol, shikimate, antheraxanthin, zeaxanthin, β-carotene) and, more weakly, AspAT and pyruvate kinase.

Another shared response was found for a set of enzymes involved in Suc degradation and glycolysis (SuSy, PGM, PPi-PFK, aldolase, NAD-GAPDH, PEPC). In most cases, their activity correlated positively with Rha, Fuc, Tyr, Phe, Val, and galacturonate-1,4-lactone and negatively with Xyl, succinate (and less strongly with other organic acids), Glu, putrescine, ascorbate, dehydroascorbate, and the amounts of Gal, Man, Xyl, Ara, and Rha in the cell wall. Again, many of these correlations are difficult to explain as a direct causal consequence of changes in Suc degradation and glycolysis.

Comparison of Developmental Changes of Enzyme Activities and Transcripts in *S. lycopersicum* 'MM'

Information about the developmental changes of transcripts, monitored using the TOM1 arrays, is available from Carrari et al. (2006). This array was created using EST information from 26 diverse tomato cDNA libraries and includes 61 sequences whose annotation indicated that they might encode one of the enzymes investigated in this study (Carrari et al., 2006). A pairwise correlation analysis was performed to identify genes whose transcriptional regulation might contribute to the developmental changes in enzyme activity reported in this study (Supplemental Table S8). Thirty-one gene sequences out of the 61 correlated with at least one enzyme activity; these results are summarized in Table III.

Of the 31 gene sequences, only four showed a significant positive correlation with the activity (FruK, PPi-PFK, NADP-GAPDH, PEPC) of the enzyme they should encode for, while two showed negative correlations (SuSy, AspAT).

Table III. *Correlations between 31 transcripts for structural genes and 25 enzyme activities in fruit development in S. lycopersicum 'MM'*

The names of the transcripts correspond to the identifying spots on the TOM01 chip; full descriptions are available in Supplemental Table S8 as well as the genes presenting no correlation with any of the enzyme activities. Sectors corresponding to parameter pairs in which the transcript is annotated as encoding the enzyme are highlighted in gray. The bold-outlined boxes indicate where a transcript correlates with the activity of the enzyme that it encodes. The table also lists other enzyme activities with which transcripts correlate and the P values. The color code for negative correlation is as follows: red if $P < -0.01$ and orange if $-0.01 < P < -0.05$; the color code for positive correlation is as follows: light blue if $0.01 < P < 0.05$ and dark blue if $P < 0.01$. The full data matrix is provided in Supplemental Table S8.

Transcript name	Invertase	AGP	FruK	SPS	UGP	PGM	PGI	SuSy	G6PDH	PPi-PFK	ATP-PFK	Aldolase	PGK	NAD-GAPDH	NADP-GAPDH	PEPC	PK	Aconitase	NADP-IcDH	SCS	NAD-MDH	NAD-GIDH	AlaAT	AspAT	ShkDH
1-1-8.3.8.2	-0.79	-0.49	-0.03	-0.65	-0.37	-0.16	-0.79	-0.09	-0.71	-0.08	-0.28	-0.10	-0.61	-0.16	-0.05	-0.20	-0.59	0.53	0.49	-0.54	-0.10	0.72	-0.35	-0.29	-0.93
1-1-2.4.11.13	-0.19	0.49	0.43	0.36	0.16	0.82	0.93	0.48	-0.92	0.09	-0.86	0.02	0.77	0.33	0.22	-0.95	-0.38	-0.33	-0.29	0.75	0.22	-0.39	-0.94	0.93	-0.23
1-1-3.3.13.8	-0.58	0.12	0.42	0.23	0.10	0.84	-0.97	0.41	-0.91	0.10	0.57	0.01	0.99	0.24	0.16	0.59	-0.76	-0.47	-0.81	0.55	0.16	-0.67	0.72	0.42	-0.49
1-1-1.1.7.16	-0.52	-0.20	-0.03	-0.15	-0.09	-0.21	-0.33	-0.04	-0.31	-0.06	-0.23	-0.06	-0.27	-0.04	-0.01	-0.10	-0.38	0.47	0.38	0.56	-0.11	-0.41	-0.22	-0.14	-0.56
1-1-3.2.4.10	0.12	0.10	0.04	0.23	0.16	0.10	0.33	0.07	0.18	0.04	0.10	0.05	0.80	0.07	0.13	0.06	0.09	-0.61	0.49	0.45	0.00	0.53	0.08	0.04	0.14
1-1-6.4.20.20	0.63	0.29	0.01	0.61	0.11	0.01	0.16	0.03	0.22	0.04	0.23	0.17	0.06	0.04	0.01	0.09	0.33	-0.65	-0.12	0.93	0.06	0.53	0.20	0.13	0.67
1-1-7.2.2.6	0.86	-0.20	-0.17	-0.13	-0.04	-0.23	-0.33	-0.18	-0.36	-0.06	-0.56	-0.10	-0.09	-0.13	-0.18	-0.38	-0.90	0.92	0.11	-0.77	-0.18	0.81	-0.45	-0.61	0.69
1-1-3.1.20.1	0.23	-0.26	-0.03	-0.41	-0.21	-0.68	-0.43	-0.06	-0.40	-0.22	-0.41	-0.62	-0.32	-0.66	-0.04	0.95	-0.56	-0.49	0.55	-0.44	-0.02	0.56	-0.85	0.82	-0.89
1-1-3.4.16.6	0.81	-0.22	0.00	-0.31	-0.01	-0.02	-0.04	0.00	-0.03	0.00	-0.68	-0.01	-0.22	0.00	0.00	-0.02	-0.31	0.06	0.28	-1.00	0.00	-0.31	-0.27	-0.03	-0.48
1-1-5.1.11.21	-0.81	-0.06	-0.78	-0.03	-0.07	-0.88	-0.88	-0.52	-0.58	-0.23	-0.14	-0.04	-0.56	-0.18	-0.18	-0.64	-0.33	-0.81	-0.72	0.69	-0.18	-0.49	-0.09	-0.18	-0.38
1-1-7.1.8.9	-0.40	-0.20	-0.15	-0.34	-0.30	-0.01	-0.42	-0.16	-0.26	-0.25	-0.27	-0.30	-0.60	-0.17	-0.34	-0.23	-0.30	0.56	-0.32	-0.20	-0.10	-0.72	-0.17	-0.10	-0.43
1-1-1.2.13.14	-0.88	0.32	0.06	0.53	0.06	0.11	0.25	0.10	0.26	0.03	0.31	0.03	0.14	0.03	0.00	0.20	0.31	-0.39	-0.26	-0.46	0.02	0.37	0.13	0.08	0.45
1-1-7.3.4.18	-0.15	-0.75	0.18	-0.46	0.37	0.12	0.01	0.26	0.11	0.26	-0.30	0.81	0.10	0.34	0.23	0.47	0.94	-0.23	-0.02	-0.15	0.37	0.38	-0.73	0.77	0.98
1-1-3.4.13	-0.30	-0.38	-0.84	-0.75	-0.92	-0.68	0.60	-0.75	0.89	-0.83	-0.25	-0.63	0.48	-0.70	-0.90	-0.59	-0.45	0.91	-0.06	-0.02	-0.47	0.95	-0.38	-0.22	-0.54
1-1-4.2.12.10	0.49	-0.22	0.01	-0.53	-0.18	-0.29	-0.34	-0.03	-0.28	-0.14	-0.18	-0.51	-0.20	-0.40	-0.01	-0.64	-0.26	-0.58	0.60	-0.42	-0.01	0.85	-0.42	-0.66	-0.53
1-1-1.3.1.20	0.86	-0.77	0.04	-0.77	0.88	0.26	0.42	0.15	0.54	0.29	-0.60	0.56	0.97	0.43	0.28	0.18	-0.89	-0.08	-0.19	-0.95	0.51	0.91	-0.59	0.76	-0.68
1-1-6.4.19.19	-0.74	0.41	0.30	0.62	0.22	0.46	-0.99	0.47	-0.90	0.12	0.27	0.05	0.35	0.24	0.05	0.78	0.91	-0.77	-0.35	0.14	-0.76	0.27	0.44	-0.81	
1-1-3.2.9.19	0.91	0.18	0.02	0.42	0.01	0.02	0.00	0.01	0.00	0.01	0.72	0.17	0.06	0.01	0.01	0.04	0.02	0.11	-0.46	-0.20	-0.72	0.05	0.03	0.43	0.19
1-1-8.4.6.9	0.60	0.30	0.08	0.48	0.08	0.01	0.15	0.11	0.09	0.06	0.58	0.43	0.05	0.13	0.23	0.18	0.32	1.00	-0.28	0.74	0.11	0.43	0.45	0.36	0.54
1-1-6.4.11.11	-0.45	0.25	0.02	0.42	0.02	0.11	0.27	0.05	0.43	0.00	0.64	0.00	0.20	0.03	0.00	0.10	0.97	-0.21	-0.07	0.87	0.01	-1.00	0.51	0.26	-0.66
1-1-3.3.11.20	-0.78	0.03	0.03	0.15	0.00	0.06	0.08	0.03	0.20	0.00	0.22	0.01	0.13	0.01	0.00	0.12	0.45	-0.52	-0.31	0.68	0.01	0.51	0.18	0.07	0.75
1-1-5.4.11.11	0.59	-0.71	-0.08	-0.62	-0.13	-0.04	-0.13	-0.17	-0.21	-0.07	0.93	-0.34	-0.03	-0.17	-0.26	-0.40	-1.00	0.66	0.02	-0.78	-0.12	0.82	-0.71	-0.83	0.68
1-1-6.4.11.16	-0.79	0.66	0.14	0.70	0.14	0.06	0.03	0.26	0.14	0.14	0.56	0.25	0.04	0.13	0.04	0.46	0.37	-0.73	-0.10	-0.22	0.05	0.37	0.17	0.26	0.44
1-1-4.4.3.16	0.89	-0.12	0.00	-0.37	-0.08	-0.11	-0.22	-0.01	-0.15	-0.05	-0.08	-0.22	-0.15	-0.11	0.00	-0.23	-0.10	-0.82	0.59	-0.67	0.00	-0.63	-0.15	-0.18	-0.27
1-1-4.3.6.2	-0.69	0.64	0.48	0.44	0.03	-0.49	-0.72	0.45	-0.68	0.22	-0.51	0.13	-0.08	0.46	0.87	0.31	-0.24	-0.49	-0.68	0.43	0.68	-0.20	-0.13	-0.42	-0.16
1-1-6.3.4.13	0.31	0.55	-0.20	-0.90	-0.19	-0.93	-0.55	-0.48	-0.98	-0.02	0.03	-0.07	0.65	-0.33	-0.38	-0.67	0.18	0.02	0.16	0.98	-0.09	0.04	0.17	0.11	0.22
1-1-8.2.11.11	-0.98	-0.07	-0.02	-0.23	-0.01	-0.02	-0.18	-0.03	-0.17	0.00	-0.32	-0.02	-0.12	-0.01	-0.03	-0.09	-0.44	0.45	0.39	-0.26	-0.01	-0.86	-0.19	-0.09	-0.85
1-1-6.4.19.11	0.69	-0.08	-0.15	-0.33	-0.24	-0.94	-0.44	-0.15	-0.27	-0.60	-0.05	0.91	-0.30	-0.82	-0.05	-0.88	-0.06	-0.07	-0.46	-0.70	-0.03	-0.53	-0.26	-0.65	-0.10
1-1-4.1.20.9	-0.93	-0.74	-0.04	-0.95	-0.59	-0.18	-0.96	-0.15	0.96	-0.11	-0.84	-0.12	0.88	-0.26	-0.14	-0.26	0.74	0.11	0.52	-0.14	-0.13	0.42	-0.95	-0.48	0.42
1-1-3.2.18.15	-0.49	0.86	-0.02	-0.89	-0.75	-0.11	-0.78	-0.11	-0.69	-0.21	-0.82	-0.31	-0.70	-0.26	-0.20	-0.13	-0.92	0.22	0.27	-0.66	-0.26	0.57	-0.68	-0.58	0.78
1-1-7.1.4.17	-0.72	-0.04	-0.06	-0.20	-0.02	-0.10	-0.44	-0.05	-0.31	-0.02	-0.30	-0.02	-0.59	-0.02	-0.05	-0.08	-0.39	0.28	-0.82	-0.30	-0.01	-0.67	-0.24	-0.03	-0.64

This comparison could be complicated by the occurrence of gene families. Our measurements of enzyme activity provide information about the summed activities of all family members. The comparison with transcripts assumes that all of the major transcripts are present on the array and that there are no reciprocal changes in the expression of different family members. The array was generated from EST sequences from fruit libraries, so it is probable that most or all major family members are represented on the array. For some cases, the array contained a family of sequences that were annotated as encoding a given enzyme. In such cases, the enzyme activity correlated with one or none of the transcripts.

We also investigated the correlations between this set of 31 transcripts and all of the other enzyme activities. Of the 775 comparisons, 118 showed a significant correlation, with a mix of positive and negative correlations. This contrasts with the large predominance of positive correlations between enzyme activities. Interestingly, the frequency distribution was highly nonnormal, with a high number of the transcripts showing no significant correlation (30) or only one correlation (11; $P < 0.05$) with an enzyme activity but a small number of transcripts showing correlations to a large number of enzyme activities (three correlated with six to eight, and four with nine to 13, of the 25 enzymes; Table III; Supplemental Table S8). Of these, four belonged to the set of transcripts that correlated with the activity of the enzyme that they encoded (Table III), including genes annotated to encode FruK, PEPC, SuSy, and AspAT.

DISCUSSION

There have been several small-scale studies of the developmental changes of enzyme activities that are involved in starch or Suc metabolism (Robinson et al., 1988; Yelle et al., 1988) and a larger study of 11 glycolytic enzymes (Obiadalla-Ali et al., 2004) in tomato fruit. More recently, these studies of enzyme activities have been complemented by proteomic analyses during fruit ripening (Rose et al., 2004; Faurobert

et al., 2007). We have now investigated the activities of 28 enzymes during tomato fruit development, located in most of the major pathways in central metabolism. The developmental changes of these enzymes in two modern *S. lycopersicum* cultivars ('M82' and 'MM') were compared with the changes in a wild relative, *S. pennellii*, which differs from the modern cultivars in being much smaller, containing higher levels of organic acids and slightly lower sugars, and remaining green at maturity.

Enzyme Activities in Developing Fruits of *S. lycopersicum* Cultivars

In the two *S. lycopersicum* cultivars, most enzyme activities decrease during fruit development (Fig. 2). While there were some differences between cultivars, this may be at least partly due to differences in the rate of fruit development. We have expressed enzyme activities on a fresh weight basis. The general trend to a decrease may be at least partly due to vacuole expansion during earlier stages of the ripening process. There are nevertheless clear differences between the responses of different types of enzyme. Overall, the capacity for Suc hydrolysis to reducing sugars remains high or increases, the capacity for Suc synthesis remains high, and the capacity for the use of hexose sugars, glycolysis, and the tricarboxylic acid cycle decreases strongly during fruit development. A similar general decrease for enzymes from Suc breakdown, starch synthesis, and glycolysis was found in *S. lycopersicum* 'MicroTom' (Obiadalla-Ali et al., 2004) and in cherry tomato (Faurobert et al., 2007).

Very large decreases of activity were found for three enzymes (SuSy, FruK, GlcK) that are required to mobilize Suc and reducing sugars. In contrast, invertase activity remained high. This resembles earlier result of Obiadalla-Ali et al. (2004) for two further cultivars and the pattern seen in proteomics studies with cherry tomato, where FruK abundance decreased and several isoforms of invertase increased (Faurobert et al., 2007). However, the overlap between proteins measured in the previous and current studies and the varietal differences still prevent a comprehensive comparison. Invertase serves to convert Suc into hexoses (Nguyen-Quoc and Foyer, 2001). The decrease of GlcK and FruK activity and the maintenance of invertase activity are accompanied by a progressive increase of hexoses and decline of Suc as tomato fruits mature (Ho, 1984; Yelle et al., 1991; Carrari et al., 2006).

Activities of enzymes for Suc synthesis (especially SPS) were substantial in young fruits and remained relatively high during ripening. This is in agreement with published studies, in which [^{14}C]Glc was used to measure fluxes. These showed that Suc synthesis occurs at high rates at all stages of the ripening process (Carrari et al., 2006), resulting in a "futile cycle" of Suc breakdown and synthesis (Nguyen-Quoc and Foyer, 2001; Rontein et al., 2002). AGP activity decreased

3-fold during fruit development. Starch may serve as a temporary store of carbon. Simultaneous synthesis and degradation of starch have been reported at several stages of tomato fruit development (N'tchobo et al., 1999). Futile cycles of Suc and starch turnover are also found in other growing storage organs (Hill and ap Rees, 1994; Geigenberger and Stitt, 2000; Geigenberger et al., 2004). They may allow sensitive regulation of flux by mediating an alternation between transient storage and remobilization depending on the momentary influx of photoassimilates (Geigenberger et al., 1994, 2004).

There was a general decrease of the activities of enzymes in glycolysis and the tricarboxylic acid cycle during fruit ripening. This included a very large decrease of PEPC activity, which is required for net synthesis of organic acids, and smaller changes of many other enzymes. The labeling experiment of Carrari et al. (2006) showed that glycolytic flux is maintained, and may even increase, between 35 and 49 DAA. It appears that this occurs independently of developmental changes in the maximal activities of enzymes from these pathways. Enzymes involved in nitrogen metabolism remained high or increased relative to the activities of enzymes in central carbon metabolism. This resembles the changes of protein levels of enzymes involved in nitrogen metabolism reported by Faurobert et al. (2007) and is consistent with the reported increase in flux to amino acids between 35 and 49 DAA (Carrari et al., 2006).

Differing Developmental Changes of Enzyme Activities in Fruits of *S. pennellii*

A different picture emerged in *S. pennellii* (Fig. 2), where most enzyme activities remained stable or even rose during fruit development. Particularly marked increases of activity were found for SuSy, UGP, PGM, SPS, ATP-PFK, and enzymes in nitrogen metabolism, especially AlaAT and shikimate DH. There was also a general increase of the activities of all enzymes in the tricarboxylic acid cycle in the later stages of fruit development. The only enzyme to show a marked and sustained decrease of activity during ripening was AGP.

When young (35–42 DAA) and mature *S. pennellii* fruits are compared, there is a shift away from starch synthesis and toward Suc turnover, glycolysis, and metabolism of organic acids. In contrast to *S. lycopersicum*, the capacity of enzymes in these central metabolic pathways is maintained and even increased during fruit maturation in the wild relative. This may reflect the fact that *S. pennellii* fruits continue to grow until maturity. *S. lycopersicum* fruits complete physical growth by 42 to 49 DAA, and the subsequent stages involve metabolic transformations but no major net growth of the fruit (Fig. 1).

These differences in enzyme profiles explain, at least qualitatively, some of the previously reported differences in the metabolic composition between *S. lycopersicum* and *S. pennellii*, including the higher levels of organic

acids, especially malate, higher levels of shikimate, and slightly lower levels of reducing sugars (Schauer et al., 2006). On the other hand, a decrease in the capacity for starch accumulation may be a common feature of fruit development in tomato and its wild relatives.

Enzyme Activity Profiles Are Diagnostic for the Stage of Development and the Genotype

The developmental profiles of enzyme activities during development in *S. lycopersicum* cultivars and *S. pennellii* were sufficiently characteristic to allow them to be used to classify fruits according to the genotype and the stage of development (Fig. 3; Table I). Principal component analysis of the two *S. lycopersicum* cultivars separated the samples corresponding to the different developmental stage, with samples from one cultivar overlapping those of the other cultivar. Clustering of enzyme activities identified three main groups of samples that corresponded with three phases of fruit development. This contrasted to *S. pennellii*, which showed a very different separation in the principal component analysis, with the young fruit resembling mid-stage *S. lycopersicum* fruit and a completely different trajectory during maturation. Clustering of the enzyme activities nevertheless identified three main groups of fruit samples, which again corresponded well with three phases of *S. pennellii* fruit development. These were different from the developmental stages in the modern tomato cultivars.

Enzyme Activities Change in a Coordinated Manner during Development

Enzyme activities change to a varying extent and at different times during development, and the response differs between *S. lycopersicum* cultivars and *S. pennellii*. We performed a global correlation analysis in each genotype to identify pairs and larger sets of enzymes that show a particularly coordinated response in a given genotype. We then compared the resulting correlation matrices to learn whether any of these coordinated responses are shared between the two cultivars and, in particular, between the modern cultivars and the wild species.

At a cutoff of $P_{adj} < 0.05$, 65% and 82% of the enzyme pairs changed in a correlated manner during fruit development in *S. lycopersicum* 'M82' and *S. lycopersicum* 'MM', respectively. At this significance level, almost all the correlations were positive (Table II). The majority of the correlations were shared between the two cultivars, underlining the coordinated nature of the developmental changes in *S. lycopersicum* fruits. Somewhat less significant correlations were detected in *S. pennellii* (46% of the enzyme pairs), but, of these, the majority were shared with one or both of the *S. lycopersicum* cultivars (Fig. 5). This overlap is striking because many enzymes show opposing changes during fruit development in *S. pennelli* compared with *S. lycopersicum*. These results indicate that basic regulatory programs that generate these coordi-

nated changes are operating on both of these species, but the developmental timing of these programs has been changed.

Coordinated changes of the activities of many enzymes may be required to allow changes in flux through a pathway. It is well established that changes of 2-fold or more in the activity of single enzymes often have little or no effect on flux, even though they may have larger effects on the levels of metabolic intermediates (Stitt and Sonnewald, 1995; Geigenberger et al., 2004; Stitt et al., 2010).

Intriguingly, some enzymes that would usually be assigned to the same metabolic pathway show differing responses during fruit development. For example, invertase shows a remarkably different developmental response to SuSy, which is the other enzyme that can mobilize Suc. Invertase also shows a very different response to GlcK and FruK, which are required to utilize the reducing sugars that are produced by invertase. This is consistent with the proposal that the main role of invertase during tomato fruit development may be to generate reducing sugars that are stored in the vacuole (Nguyen-Quoc and Foyer, 2001), whereas the SuSy functions to mobilize Suc, and FruK and GlcK may be involved in both functions.

Changes in gene expression will make a contribution to determining enzyme activities, which in turn will play a major role in determining the metabolic profile. Analysis of a large metabolite profiling data set for developing fruit of *S. lycopersicum* 'MM' has already revealed many correlations between metabolites (Carrari et al., 2006), and analysis of a large transcript profiling data set for developing fruit of *S. lycopersicum* 'MM' has revealed many correlations between transcripts (Carrari et al., 2006). We took advantage of the fact that our measurements of enzymes in *S. lycopersicum* 'MM' used the same material as that used for these analyses of metabolites and transcripts to investigate connectivity between all three functional levels during tomato fruit development.

Connectivity between Enzyme Activities and Metabolites

As already discussed, there is a high frequency of correlations between enzyme activities, and these correlations are almost all positive (Fig. 6; Supplemental Fig. S3). The combined correlation matrix between nzymes and metabolites has a slightly lower frequency of correlations between metabolite-enzyme pairs than between enzyme-enzyme pairs or metabolite-metabolite pairs, and many of the correlations between metabolites and enzymes are negative (Fig. 6). Metabolites also show many correlations with each other, with almost equal numbers of positive and negative correlations (Carrari et al., 2006). The negative correlations between enzymes and metabolites are presumably generated because increased activity of an enzyme can lead to a decrease in the levels of metabolites that are located downstream of the enzyme, whereby this can be due to its position in a pathway or

in a regulatory loop. It can be envisaged that this, in turn, generates the mix of negative and positive correlations that is seen in metabolite profiles.

The changes of individual metabolites, however, cannot be readily explained from the changes of individual enzyme activities. Our data matrix contained many examples of metabolite-enzyme pairs where the metabolite was the direct substrate or product of the enzyme. Among these there were no positive correlations and only two negative correlations involving α-ketoglutarate and AlaAT or AspAT. A similar complexity remained when the matrix was analyzed at the level of pathways. For example, even though fruit development was associated with a general decrease of the levels of many glycolytic enzymes, most organic acids stabilize or increase during the later stages of fruit development in *S. lycopersicum* 'MM' (Carrari et al., 2006). This is reflected in the negative correlations between ATP-PFK and citrate, aconitate, 2-oxoglutarate, and malate and the negative correlations between succinate and several other enzymes for Suc degradation and glycolysis (Fig. 6). This implies that the metabolic profile is generated by an interaction between many enzymes, leading to a complex and not easily predictable situation when many enzymes are changing simultaneously. As another example, a set of enzymes involved in Suc degradation and glycolysis (SuSy, PGM, PPi-PFK, aldolase, NAD-GAPDH, PEPC) that were negatively related to succinate showed opposing correlations to metabolites that are located upstream of them (e.g. positive correlations to some sugars and negative correlations to others). There is also no obvious explanation why these enzymes correlate positively with minor amino acids like Phe, Tyr, Ile, and Val, but negatively with Glu, from which the amino group for the synthesis of these amino acids is derived, or for why they correlate with changes in the levels of different sugars in the cell wall residue.

The level of a metabolite presumably depends on the balance between its synthesis and consumption. It is possible that the negative correlations between glycolytic enzymes and organic acids noted in the previous paragraphs could be resolved by extending the analysis to include pathways that consume organic acids, like the mitochondrial electron transport chain and biosynthetic processes like protein synthesis. However, the highly coordinated changes of many enzyme activities will, paradoxically, make it more difficult to predict the impact on metabolite levels. In the extreme case, increasing the activities of all the enzymes in a given sector of metabolism could increase fluxes without having any effect at all on the levels of the metabolic intermediates (Kacser and Acerenza, 1993). Our joint analysis of enzyme activities and metabolites indicates that the metabolite profile is an emergent property that cannot be readily predicted from enzyme activities alone. Knowledge of the topology of the metabolic network will also be required, including not only information about the location of the enzymes but also about their regulatory properties and how these link enzymes at different sites in the metabolic network.

Relation between Transcript Levels and Enzyme Activities

Analysis of a large transcript profiling data set for developing fruit of *S. lycopersicum* 'MM' revealed many correlations between the levels of different transcripts (Carrari et al., 2006). When this data set was combined with our data set for enzyme activities, the connectivity between the developmental changes of transcripts and enzymes was rather limited. Of 31 comparisons between a transcript and an encoded enzyme, we found only four positive correlations and two negative correlations. This comparison could be complicated by the occurrence of gene families. As the array was generated from EST sequences from fruit libraries, it is probable that most or all major family members are represented on the array. Our measurements of enzyme activity provide information about the summed activities of all of the family members, and the comparison with transcripts assumes that all of the major transcripts are present on the array and that there are no reciprocal changes in the expression of different family members. These results are nevertheless in general agreement with other studies that have found short-term changes in responses of transcripts, and these enzyme activities are almost unrelated, and long-term changes some show agreement (Gibon et al., 2004, 2006; Morcuende et al., 2007; Osuna et al., 2007; Usadel et al., 2008). Combining this result with the analysis of the connectivity between enzyme activities and metabolites (see above) indicates that, at least for tomato fruit development, there is a low level of connectivity between transcript levels and maximum enzyme activities and even less between enzyme activities and metabolite levels. This may be a consequence of the complex networks that link events at these different functional levels.

In conclusion, our analyses of enzyme activity profiles in modern cultivars and in the wild relative *S. pennellii* lead to two main conclusions. First, the developmental changes of enzyme activities in *S. pennellii* differ markedly from those in modern tomato cultivars. This provides an underlying explanation for the large differences in metabolite profiles between *S. pennellii* and modern cultivars and for the large variation in metabolite levels in near isogenic lines created by crosses between *S. pennellii* and *S. lycopersicum* 'M82'. Second, there are complex connectivities between individual enzymes but surprisingly little connectivity between transcript levels and the activities of the coded enzyme and between enzyme activities and the metabolite profile during tomato fruit development. Analysis of QTLs for enzyme activities in near isogenic lines could provide further insights into the complex genetic architecture that controls metabolite contents in tomato.

MATERIALS AND METHODS

Materials

Inorganic compounds were purchased from Merck and organic compounds from Sigma except ethanol (Merck) and NAD$^+$, NADH, NADP$^+$, NADPH, and phospho*enol*pyruvate (Roche). Enzymes for analysis were purchased from Roche except phosphoglycerokinase and glycerokinase (Sigma-Aldrich). UMP-kinase was overexpressed and purified as described by Serina et al. (1995). The clone encoding for the UMP-kinase is a generous gift from Octavian Barzu (Institut Pasteur, Paris).

Plant Material and Growth

Solanum lycopersicum 'M82' seeds were kindly provided by Stephan Krueger (Max Planck Institute of Molecular Plant Physiology). Seeds of *Solanum pennellii* (LA0716) were obtained from true-breeding monogenic stocks (CM Rick Tomato Genetics Resource Center, University of California, Davis).

All seeds were germinated on Murashige and Skoog medium (Murashige and Skoog, 1962) containing 2% (w/v) Suc and were grown in a growth chamber with 500 μmol photons m^{-2} s^{-1} at 25°C temperature under a 12-h-light/12-h-dark regime. After 2 weeks, seedlings were transplanted into individual 20-cm pots containing 12 g of Osmocote exact (5–6 M) used as fertilizer in mixed tomato soil consisting of two parts standard potato soil, one part quartz sand (grain size, 0.3–0.8 mm), and one part vermiculite (fine grain). These pots were transferred to the greenhouse, where they were grown in parallel under long-day conditions with a minimum of 250 μmol photons m^{-2} s^{-1} at 20°C to 24°C temperature and 60% to 70% relative humidity under a 16-h-light/8-h-dark regime. Samples of *S. lycopersicum* 'MM' from 28 to 70 DAA were grown and sampled under the conditions described by Carrari et al. (2006).

Fruits were harvested at different stages of development based on their color for M82 and/or on the number of DAA for other genotypes. Individual flowers were tagged at anthesis to accurately follow fruit ages through development. As the attachment of *S. pennellii* peduncle to the stem is very fragile, tagging of individual flowers was only possible for a few flowers. To avoid peduncle breaking, fruit development in *S. pennellii* was followed by photographing plants to determine the DAA for each fruit in conjunction with determination of the increase in fruit size. Fruit height and diameter were measured with a caliper on fruits either still attached to the vine or directly after harvesting. Tomato fruits were harvested at the middle (*S. lycopersicum* 'MM') or the end (*S. lycopersicum* 'M82', *S. pennellii*) of the light period. To follow tomato fruit development, fruits were harvested at 7-d intervals between 7 DAA (*S. lycopersicum* 'M82') or 28 DAA/d after flowering (DAF; *S. lycopersicum* 'MM', *S. pennellii*) to 70 DAA/DAF, which represents the ripe stage of fruit development. For the red-fruited *S. lycopersicum* cultivars, the period of 28 to 70 DAA covers the full transition from green to fully ripe red fruits. All fruits were weighted immediately upon harvesting and cut in two parts. The pericarp was then separated from the placental tissue, immediately frozen in liquid N$_2$, and stored at −80°C. At each time point, with the exceptions of 28 and 70 DAA, five to 10 replicate samples from a single separate fruit were collected.

Sample Extraction

For determining enzyme activities, each sample was ground to a fine powder under liquid nitrogen and stored at −80°C until use. Samples (approximately 20 mg fresh weight) were weighed out at −180°C and extracted by addition of 10 mg (w/v) polyvinylpolypyrrolidone and vigorous shaking in 300 μL of ice-cold extraction buffer. The latter was modified from Gibon et al. (2004) with higher amounts of glycerol (20%, v/v) and Triton X-100 (2%, v/v). The crude extract was centrifuged for 10 min at 20,000g and 4°C. Aliquots of the extract were further diluted to a final dilution of 1 mg fresh weight in 150 to 15,000 μL of extraction buffer for use in different enzyme assays (Supplemental Table S2). Enzymes were measured immediately or after snap freezing small aliquots (50–100 μL) at −180°C, storage at −70°C, and rethawing.

Enzyme Assays

Assay mixes and extracts were transferred to microtiter plates using a Perkin-Elmer Multiprobe II. Reactions on plates were started and stopped using a Perkin-Elmer EP3 equipped with a 50-μL head. Determinations of the reactions were measured with Bio-Tek Elx800 and Elx808 and Synergy microtiter plate readers.

Continuous Assays

Triose phosphate isomerase (TPI) and PGI were assayed as described by Burrell et al., 1994) and Cross et al. (2006), respectively. PGM and NAD-MDH were assayed according to Gibon et al. (2009).

Stopped Assays

Acid invertase was assayed in the direction of Suc breakdown to Fru and Glc. Extracts were incubated in a solution containing 50 mM acetate/KOH, pH 5.0, and 20 mM Suc, and the reaction was stopped with 20 μL of 0.5 M NaOH after 20 min (blank) or 40 min (maximal activity). After neutralization, products were determined (Supplemental Fig. S2B) by preincubating at 30°C with 60 mM ATP, 50 mM NADP, and 2 units mL^{-1} G6PDH, followed by the addition of 1 unit mL^{-1} hexokinase and 1 unit mL^{-1} PGI. A_{340} was followed until the signal stabilized.

Stopped assays were coupled to a glycerol-3-phosphate cycle as described by Gibon et al. (2004) with an optimized incubation time of 60 min for tomato fruit samples.

AGP, NAD-GAPDH, NADP-GAPDH, PPi-PFK, PK, and SPS were adapted from Gibon et al. (2004). ATP-PFK, UGP, and SuSy were adapted for tomato fruit measurements (Supplemental Table S1) from the method described by Keurentjes et al. (2008). Succinyl-CoA ligase was adapted for tomato fruit measurements (Supplemental Table S1) from the method described by Studart-Guimarães et al. (2005).

PGK was adapted from Burrell et al. (1994) and was measured in the forward direction from the transfer of a phosphate from ATP to 3-phosphoglycerate, resulting in 1,3-biphosphoglycerate and ADP. Extracts as well as dihydroxyacetone phosphate (DHAP) standards, prepared in the extraction buffer and ranging from 0 to 1 nmol, were incubated in a solution containing 100 mM Tricine/KOH, pH 8, 5 mM MgCl$_2$, 10 mM KCl, 0.5 mM EDTA, 0.5 mM 3-phosphoglycerate, 1 unit of NAD-GAPDH, 0.2 unit of glycerol-3-phosphate dehydrogenase, 0.5 mM dithiothreitol, 30 μM NADH, and 0 (blank) or 0.5 mM (maximal activity) ATP. The reaction was started by the addition of 3-phosphoglycerate and stopped with 20 μL of a solution containing 0.5 M HCl and 0.1 M Tricine/KOH pH 8.5.

Fru-1,6-bisP aldolase was adapted from Haake et al. (1998) and assayed in the direction of breaking the Fru-1,6-bisP down into glyceraldehyde 3-phosphate and DHAP. Extracts as well as DHAP standards, prepared in the extraction buffer and ranging from 0 to 1 nmol, were incubated in a solution containing 100 mM Tricine/KOH, pH 8.5, 5 mM MgCl$_2$, 1 mM EDTA, 2 units mL^{-1} glycerol-3-phosphate dehydrogenase, 1 unit mL^{-1} TPI, 5 mM NADH, and 0 (blank) or 5 mM (maximal activity) Fru-1,6-bisP. The reaction was started by the addition of TPI and stopped with 20 μL of a solution containing 0.5 M HCl and 0.1 M Tricine/KOH, pH 8.5.

For all assays, the stopped assay was neutralized and glycerol-3-phosphate was measured as described by Gibon et al. (2002).

Stopped assays coupled to a NADPH cycle were modified from Gibon et al. (2004). In these assays, NADPH is formed as a product and is determined via an enzymatic cycle between G6PDH and phenazine ethosulfate (PES). G6PDH catalyzes a G6P-mediated conversion of NADP$^+$ into NADPH,H$^+$, and PES converts NADPH,H$^+$ back to NADP$^+$. The reduced PES is reoxidized by 3-(4,5-dimethylthiazol-2-yl)-2,5-diphenyltetrazolium bromide (MTT), leading to accumulation of reduced MTT, which is measured spectrophotometrically.

GlcK, FruK, G6PDH, NADP-IcDH, and ShkDH were assayed as described by Gibon et al. (2004).

The aconitase assay was adapted from Jenner et al. (2001) and measured in the direction of the hydration of aconitate to form isocitrate. Extracts as well as isocitrate standards, prepared in the extraction buffer and ranging from 0 to 1 nmol, were incubated in a solution containing 100 mM Tricine/KOH, pH 7.5, 1 mM MgCl$_2$, 0.5 mM NADP, 0.2 unit NADP-IcDH, and 0 (blank) or 1 mM (maximal activity) aconitate. The reaction was started by the addition of NADP-IcDH.

After 60 min of incubation, conditions were optimized for tomato fruit samples and all reactions were stopped with 20 μL of 0.5 M NaOH. To destroy unreacted NADP$^+$, the plates were mixed and centrifuged (2 min at 3,500g), sealed using an adhesive aluminum foil, and heated at 95°C for 5 min. After cooling down, 20 μL of a solution containing 0.5 M HCl and 0.1 M

Tricine/KOH, pH 8.5, was added to adjust the pH to 8.5. NADPH was determined by a method modified from Gibon et al. (2002) in the presence of 3 units mL^{-1} G6PDH grade I, 100 mM Tricine/KOH, pH 9.0, 5 mM $MgCl_2$, 4 mM EDTA, 0.1 mM PES, 0.6 mM MTT, and 3 mM Glc-6-P. The absorbance was read at 570 nm and 30°C until the rates were stabilized. The rates of reactions were calculated as the increase of the absorbance in mOD min^{-1}.

Stopped Assays Coupled to a NAD⁺ Cycle

The basis for these assays is the enzymatic cycle between ADH and PES. ADH catalyzes an ethanol-mediated conversion of NAD^+ into NADH,H⁺, and PES converts NADH,H⁺ back into NAD^+ and simultaneously reduces MTT, analogous to the NADPH cycle (see above).

AlaAT, AspAT, fumarase, NAD-GlDH, and PEPC were assayed as described by Gibon et al. (2004). The reactions were incubated for 60 min (conditions optimized for tomato fruit samples) and stopped by 20 μL of 0.5 M NaOH. To destroy unreacted NADH, the plates were mixed and centrifuged (2 min at 3,500g), sealed using an adhesive aluminum foil, and heated at 95°C for 10 min. After cooling down, 20 μL of a solution containing 0.5 M HCl and 0.1 M Tricine/KOH, pH 8.5, was added to adjust the pH to 8.5. NAD^+ was measured in the presence of 6 units mL^{-1} ADH, 100 mM Tricine/KOH, pH 8.5, 4 mM EDTA, 0.1 mM PES, 0.6 mM MTT, and 500 mM ethanol. The absorbance was read at 570 nm and 30°C until the rates were stabilized. The rates of reactions were calculated as the increase of the absorbance in mOD min^{-1}.

Graphical Visualization and Heat Maps

All graphs and heat maps were created using Sigma Plot 10 (Systat Software), Microsoft Powerpoint/Excel (Microsoft Office 2007), or the R 2.6.1 software (R Development Core Team, 2007). Heat maps, generated with R, were further processed using Adobe Photoshop 7.0 (Adobe Systems). Cluster trees drawn in the heat maps were generated using hierarchical cluster analyses (HCA) with the average linkage cluster algorithm (UPGMA; compare with Mirkin, 1996).

Statistical Data Analysis and Classification

Statistical analyses were implemented in and performed with R, or available R functions were used. For some cases (e.g. t test), the available Microsoft Excel (Microsoft Office 2007) functions have been used.

The parametric two-sample t test for the difference in mean was performed two sided using the available R function and executed with equal or unequal variance analyzed using Hartley's F_{max} test (Hartley, 1950; Sokal and Rohlf, 1995). The obtained P values were adjusted for multiple testing by Bonferroni correction (P_{adj}). To avoid the influence of outliers, one-dimensional outliers were detected and removed by a boxplot approach performed with standard parameters as implemented in R. Data points that lie beyond the extremes of the whiskers are treated as outliers and were removed from further analysis.

Correlation analyses among all enzyme activities were performed as parametric Pearson's product-moment correlation (r) in a robust way. For this, two-dimensional outliers were detected by calculating the robust Mahalanobis distance based on a robust estimate of the center and the covariance with the minimum volume ellipsoid estimator (Rousseeuw and Leroy, 2003). As the observed distances are approximately χ^2 distributed with p degrees of freedom (χ^2_p), outliers were detected using the 97.5% quantile with 2 degrees of freedom and removed from pairwise correlation analyses. To adjust P values (P_{adj}) from correlation analysis for multiple comparisons, the Benjamini-Hochberg correction (Benjamini and Hochberg, 1995) was applied to control the false discovery rate. The degree centrality was calculated for each enzyme by counting the number of significant connections with adjusted $P_{adj} < 0.05$.

In the case of symmetrical correlation matrices, only the half-matrix without the diagonal was considered.

The Mantel test, as a matrix correlation between two dissimilarity matrices, was performed as parametric Pearson correlation with 9,999 bootstrap samples (Sokal and Rohlf, 1995). Fisher's exact test to estimate potential enrichments of classes (compare with Sokal and Rohlf, 1995) was executed in R.

Principal component analysis was performed as probabilistic principal component analyses with the pcaMethods package to handle missing values (Stacklies et al., 2007). The shrunk data sets for each genotype were normalized separately by calculating the ratio for each particular enzyme in each sample to the mean average activity of the corresponding enzyme in the entire

sample group at 42 DAA, the ratios were log_2 transformed, and the shrunk genotype-specific data sets were then fused. For that, enzymes measured in only one or two out of the three genotypes were excluded. The resulting fused data set contains 135 samples, corresponding to individual and genotype-specific developmental groups, and 22 enzymes with about 9.9% missing values.

All HCA were performed with the average linkage cluster algorithm (UPGMA; compare with Mirkin, 1996) on distance matrices that were generated by calculating the Euclidean distances between the samples under investigation. Correlation matrices subjected to HCA were first converted into corresponding distance matrices using the equation $1 - r$. Clustering was performed on the shrunk data sets for each genotype, and log base 2-transformed ratios were calculated for the average enzyme activity of the respective 42-DAA samples for each enzyme in each different data set. Therefore, changes in the sign of the log base 2-transformed ratios for *S. lycopersicum* 'M82' would correspond to an increase or decrease of an enzyme activity compared with the transition from fruit growth to ripening (Supplemental Fig. S3). This transition occurs slightly later in *S. lycopersicum* 'MM', but high and significant Pearson matrix correlations were found between Euclidean distance matrices generated on log base 2-transformed ratios of 42 and 49 DAA (data not shown), both for enzymes and for DAA samples ($r = 0.947$, $P <$ 1e-04 and $r = 1.0$, $P <$ 1e-04, respectively). This analysis demonstrated that a similar classification regarding enzyme and DAA can be obtained independently of the DAA used for normalization and ratio calculation. No specific transition stage could be visually detected for *S. pennellii*. Thus, the data set was normalized to 42 DAA in an identical manner as described for both tomato cultivars.

To test the validity of the obtained cluster results, data sets used in this study were bootstrapped with 999 repetitions by replacing one value by a value randomly selected from a normal distribution with the calculated mean and SD for each sample and each enzyme measured, respectively. The Euclidean distances for each generated matrix were calculated, and the resulting distance matrix was subjected to HCA as described above. The generated cluster trees were converted with R into a Newick tree format. The resulting consensus tree was generated with the consensus program of the PHYLIP package (Felsenstein, 2004) of all bootstrapped cluster trees. The validity of resulting clusters was tested by nonparametric ANOVA using the Mantel test, which was computed as Pearson's correlation between two distance matrices as described (Sokal and Rohlf, 1995) with 9,999 row and column permutations. The average matrix was computed as the mean average over all bootstrapped matrices.

Supplemental Data

The following materials are available in the online version of this article.

Supplemental Figure S1. Simplified scheme of the carbohydrate metabolism and associated reactions.

Supplemental Figure S2. Scheme of the enzyme assays.

Supplemental Figure S3. Optimization of the extraction and enzyme assay exemplarily depicted for FruK.

Supplemental Figure S4. Heat map visualization and cluster tree representation based on enzyme activities.

Supplemental Figure S5. Heat map visualization and cluster tree representation of enzyme correlations according to their activity changes during fruit development.

Supplemental Table S1. Overview of the optimized enzyme assays, their EC numbers, the abbreviations used in this work, and the principle of the assay.

Supplemental Table S2. Overview of the enzyme assays, their optimal ranges of dilution, and the dilution factors chosen for this work.

Supplemental Table S3. Comparison of the maximal enzyme activities of *S. lycopersicum* 'M82' tomato fruit pericarp harvested at different DAA.

Supplemental Table S4. Comparison of the maximal enzyme activities of *S. lycopersicum* 'MM' tomato fruit pericarp harvested at different DAA.

Supplemental Table S5. Comparison of the maximal enzyme activities of *S. pennellii* tomato fruit pericarp harvested at different DAF.

Supplemental Table S6. Overview of complete (cpl) and shrunk (shr) enzyme activity data sets for the different cultivars and species under investigation.

Supplemental Table S7. Correlation matrix between enzymes and metabolites during fruit development in *S. lycopersicum* 'MM'.

Supplemental Table S8. Correlation matrix between enzymes and transcripts during fruit development in *S. lycopersicum* 'MM'.

Supplemental Table S9. Pearson's correlation coefficient for all enzyme-metabolite pairs, where the metabolite is a direct substrate or product of the enzyme, plus the *P* value of the correlation coefficient.

ACKNOWLEDGMENTS

LITERATURE CITED

Baerenfaller K, Grossmann J, Grobei MA, Hull R, Hirsch-Hoffmann M, Yalovsky S, Zimmermann P, Grossniklaus U, Gruissem W, Baginsky S (2008) Genome-scale proteomics reveals Arabidopsis thaliana gene models and proteome dynamics. Science 320: 938–941

Baxter CJ, Carrari F, Bauke A, Overy S, Hill SA, Quick PW, Fernie AR, Sweetlove LJ (2005a) Fruit carbohydrate metabolism in an introgression line of tomato with increased fruit soluble solids. Plant Cell Physiol 46: 425–437

Baxter CJ, Sabar M, Quick WP, Sweetlove LJ (2005b) Comparison of changes in fruit gene expression in tomato introgression lines provides evidence of genome-wide transcriptional changes and reveals links to mapped QTLs and described traits. J Exp Bot 56: 1591–1604

Benjamini Y, Hochberg Y (1995) Controlling the false discovery rate: a practical and powerful approach to multiple testing. J R Stat Soc B 57: 289–300

Bertin N, Causse M, Brunel B, Tricon D, Genard M (2009) Identification of growth processes involved in QTLs for tomato fruit size and composition. J Exp Bot 60: 237–248

Brewer MT, Moyseenko JB, Monforte AJ, van der Knaap E (2007) Morphological variation in tomato: a comprehensive study of quantitative trait loci controlling fruit shape and development. J Exp Bot 58: 1339–1349

Burrell MM, Mooney PJ, Blundy M, Carter D, Wilson F, Green J, Blundy KS, Ap Rees T (1994) Genetic manipulation of 6-phosphofructokinase in potato tubers. Planta 194: 95–101

Carrari F, Baxter C, Usadel B, Urbanczyk-Wochniak E, Zanor MI, Nunes-Nesi A, Nikiforova V, Centero D, Ratzka A, Pauly M, et al (2006) Integrated analysis of metabolite and transcript levels reveals the metabolic shifts that underlie tomato fruit development and highlight regulatory aspects of metabolic network behavior. Plant Physiol 142: 1380–1396

Carrari F, Fernie AR (2006) Metabolic regulation underlying tomato fruit development. J Exp Bot 57: 1883–1897

Causse M, Duffe P, Gomez MC, Buret M, Damidaux R, Zamir D, Gur A, Chevalier C, Lemaire-Chamley M, Rothan C (2004) A genetic map of candidate genes and QTLs involved in tomato fruit size and composition. J Exp Bot 55: 1671–1685

Chaerani R, Smulders MJ, van der Linden CG, Vosman B, Stam P, Voorrips RE (2007) QTL identification for early blight resistance (Alternaria solani) in a Solanum lycopersicum × S. arcanum cross. Theor Appl Genet 114: 439–450

Cross JM, von Korff M, Altmann T, Bartzetko L, Sulpice R, Gibon Y, Palacios N, Stitt M (2006) Variation of enzyme activities and metabolite levels in 24 Arabidopsis accessions growing in carbon-limited conditions. Plant Physiol 142: 1574–1588

Cuartero J, Bolarin MC, Asins MJ, Moreno V (2006) Increasing salt tolerance in the tomato. J Exp Bot 57: 1045–1058

Eshed Y, Zamir D (1994) Introgressions from Lycopersicon pennellii can improve the soluble solids yield of tomato hybrids. Theor Appl Genet 88: 891–897

Faurobert M, Mihr C, Bertin N, Pawlowski T, Negroni L, Sommerer N, Causse M (2007) Major proteome variations associated with cherry tomato pericarp development and ripening. Plant Physiol 143: 1327–1346

Felsenstein J (2004) PHYLIP (Phylogeny Inference Package). Department of Genome Sciences, University of Washington, Seattle

Finkers R, van Heusden AW, Meijer-Dekens F, van Kan JA, Maris P, Lindhout P (2007) The construction of a Solanum habrochaites LYC4 introgression line population and the identification of QTLs for resistance to Botrytis cinerea. Theor Appl Genet 114: 1071–1080

Fraser PD, Enfissi EM, Goodfellow M, Eguchi T, Bramley PM (2007) Metabolite profiling of plant carotenoids using the matrix-assisted laser desorption ionization time-of-flight mass spectrometry. Plant J 49: 552–564

Fridman E, Carrari F, Liu YS, Fernie AR, Zamir D (2004) Zooming in on a quantitative trait for tomato yield using interspecific introgressions. Science 305: 1786–1789

Geigenberger P, Merlo L, Reimholz R, Stitt M (1994) When growing potato tubers are detached from their mother plant there is a rapid inhibition of starch synthesis, involving inhibition of ADP-glucose pyrophosphorylase. Planta 193: 486–493

Geigenberger P, Stitt M (2000) Diurnal changes in sucrose, nucleotides, starch synthesis and AGPS transcript in growing potato tubers that are suppressed by decreased expression of sucrose phosphate synthase. Plant J 23: 795–806

Geigenberger P, Stitt M, Fernie AR (2004) Metabolic control analysis and regulation of the conversion of sucrose to starch in growing potato tubers. Plant Cell Environ 27: 655–673

Gibon Y, Blaesing OE, Hannemann J, Carillo P, Hohne M, Hendriks JHM, Palacios N, Cross J, Selbig J, Stitt M (2004) A robot-based platform to measure multiple enzyme activities in *Arabidopsis* using a set of cycling assays: comparison of changes of enzyme activities and transcript levels during diurnal cycles and in prolonged darkness. Plant Cell 16: 3304–3325

Gibon Y, Pyl ET, Sulpice R, Lunn JE, Hohne M, Gunther M, Stitt M (2009) Adjustment of growth, starch turnover, protein content and central metabolism to a decrease of the carbon supply when Arabidopsis is grown in very short photoperiods. Plant Cell Environ 32: 859–874

Gibon Y, Usadel B, Blaesing OE, Kamlage B, Hoehne M, Trethewey R, Stitt M (2006) Integration of metabolite with transcript and enzyme activity profiling during diurnal cycles in Arabidopsis rosettes. Genome Biol 7: R76

Gibon Y, Vigeolas H, Tiessen A, Geigenberger P, Stitt M (2002) Sensitive and high throughput metabolite assays for inorganic pyrophosphate, ADPGlc, nucleotide phosphates, and glycolytic intermediates based on a novel enzymic cycling system. Plant J 30: 221–235

Gillaspy G, Ben-David H, Gruissem W (1993) Fruits: a developmental perspective. Plant Cell 5: 1439–1451

Giovannoni J (2001) Molecular biology of fruit maturation and ripening. Annu Rev Plant Physiol Plant Mol Biol 52: 725–749

Grumet R, Fobes JF, Herner RC (1981) Ripening behavior of wild tomato species. Plant Physiol 68: 1428–1432

Haake V, Zrenner R, Sonnewald U, Stitt M (1998) A moderate decrease of plastid aldolase activity inhibits photosynthesis, alters the levels of sugars and starch, and inhibits growth of potato plants. Plant J 14: 147–157

Hartley HO (1950) The maximum F-ratio as a short-cut test for heterogeneity of variance. Biometrika 37: 308–312

Hill SA, ap Rees T (1994) Fluxes of carbohydrate metabolism in ripening bananas. Planta 192: 52–60

Ho LC (1984) Partitioning of assimilates in fruiting tomato plants. Plant Growth Regul 2: 277–285

Jenner HL, Winning BM, Millar AH, Tomlinson KL, Leaver CJ, Hill SA (2001) NAD malic enzyme and the control of carbohydrate metabolism in potato tubers. Plant Physiol 126: 1139–1149

Jimenez-Gomez JM, Alonso-Blanco C, Borja A, Anastasio G, Angosto T, Lozano R, Martinez-Zapater JM (2007) Quantitative genetic analysis of flowering time in tomato. Genome 50: 303–315

John Goodstal F, Kohler GR, Randall LB, Bloom AJ, St Clair DA (2005) A

major QTL introgressed from wild Lycopersicon hirsutum confers chilling tolerance to cultivated tomato (Lycopersicon esculentum). Theor Appl Genet 111: 898–905

Kacser H, Acerenza L (1993) A universal method for achieving increases in metabolite production. Eur J Biochem 216: 361–367

Keurentjes JJ, Sulpice R, Gibon Y, Steinhauser MC, Fu J, Koornneef M, Stitt M, Vreugdenhil D (2008) Integrative analyses of genetic variation in enzyme activities of primary carbohydrate metabolism reveal distinct modes of regulation in Arabidopsis thaliana. Genome Biol 9: R129

Klee HJ, Hayford MB, Kretzmer KA, Barry GF, Kishore GM (1991) Control of ethylene synthesis by expression of a bacterial enzyme in transgenic tomato plants. Plant Cell 3: 1187–1193

Knapp S, Bohs L, Nee M, Spooner DM (2004) Solanaceae: a model for linking genomics with biodiversity. Comp Funct Genomics 5: 285–291

Kortstee AJ, Appeldoorn NJG, Oortwijn MEP, Visser RGF (2007) Differences in regulation of carbohydrate metabolism during early fruit development between domesticated tomato and two wild relatives. Planta 226: 929–939

Lippman ZB, Semel Y, Zamir D (2007) An integrated view of quantitative trait variation using tomato interspecific introgression lines. Curr Opin Genet Dev 17: 545–552

Liu YS, Gur A, Ronen G, Causse M, Damidaux R, Buret M, Hirschberg J, Zamir D (2003) There is more to tomato fruit colour than candidate carotenoid genes. Plant Biotechnol J 1: 195–207

Menda N, Semel Y, Peled D, Eshed Y, Zamir D (2004) In silico screening of a saturated mutation library of tomato. Plant J 38: 861–872

Mirkin B (1996) Mathematical Classification and Clustering, Vol 11. Kluwer Academic Publishers, London

Mitchell-Olds T, Pedersen D (1998) The molecular basis of quantitative genetic variation in central and secondary metabolism in Arabidopsis. Genetics 149: 739–747

Morcuende R, Bari R, Gibon Y, Zheng W, Pant BD, Blasing O, Usadel B, Czechowski T, Udvardi MK, Stitt M, et al (2007) Genome-wide reprogramming of metabolism and regulatory networks of Arabidopsis in response to phosphorus. Plant Cell Environ 30: 85–112

Mounet F, Moing A, Garcia V, Petit J, Maucourt M, Deborde C, Bernillon S, Le Gall G, Colquhoun I, Defernez M, et al (2009) Gene and metabolite regulatory network analysis of early developing fruit tissues highlights new candidate genes for the control of tomato fruit composition and development. Plant Physiol 149: 1505–1528

Mueller LA, Solow TH, Taylor N, Skwarecki B, Buels R, Binns J, Lin C, Wright MH, Ahrens R, Wang Y, et al (2005a) The SOL Genomics Network: a comparative resource for Solanaceae biology and beyond. Plant Physiol 138: 1310–1317

Mueller LA, Tanksley SD, Giovannoni JJ, van Eck J, Stack S, Choi D, Kim BD, Chen M, Cheng Z, Li C, et al (2005b) The Tomato Sequencing Project, the first cornerstone of the International Solanaceae Project (SOL). Comp Funct Genomics 6: 153–158

Murashige T, Skoog F (1962) A revised medium for rapid growth and bioassays with tobacco tissue cultures. Physiol Plant 15: 473–497

Nguyen-Quoc B, Foyer CH (2001) A role for 'futile cycles' involving invertase and sucrose synthase in sucrose metabolism of tomato fruit. J Exp Bot 52: 881–889

N'tchobo H, Dali N, Nguyen-Quoc B, Foyer CH, Yelle S (1999) Starch synthesis in tomato remains constant throughout fruit development and is dependent on sucrose supply and sucrose synthase activity. J Exp Bot 50: 1457–1463

Obiadalla-Ali H, Fernie AR, Kossmann J, Lloyd JR (2004) Developmental analysis of carbohydrate metabolism in tomato (Lycopersicon esculentum cv. Micro-Tom) fruits. Physiol Plant 120: 196–204

Osuna D, Usadel B, Morcuende R, Gibon Y, Blasing OE, Hohne M, Gunter M, Kamlage B, Trethewey R, Scheible WR, et al (2007) Temporal responses of transcripts, enzyme activities and metabolites after adding sucrose to carbon-deprived Arabidopsis seedlings. Plant J 49: 463–491

Prioul JL, Pelleschi S, Sene M, Thevenot C, Causse M, de Vienne D, Leonardi A (1999) From QTLs for enzyme activity to candidate genes in maize. J Exp Bot 50: 1281–1288

R Development Core Team (2007) R: A Language and Environment for Statistical Computing. R Foundation for Statistical Computing, Vienna

Rick CM (1976) Natural variability in wild species of Lycopersicon and its bearing on tomato breeding. Genetica Agraria 30: 249–259

Robinson NL, Hewitt JD, Bennett AB (1988) Sink metabolism in tomato

fruit. 1. Developmental changes in carbohydrate metabolizing enzymes. Plant Physiol 87: 727–730

Rontein D, Dieuaide-Noubhani M, Dufourc EJ, Raymond P, Rolin D (2002) The metabolic architecture of plant cells: stability of central metabolism and flexibility of anabolic pathways during the growth cycle of tomato cells. J Biol Chem 277: 43948–43960

Rose JK, Bashir S, Giovannoni JJ, Jahn MM, Saravanan RS (2004) Tackling the plant proteome: practical approaches, hurdles and experimental tools. Plant J 39: 715–733

Rousseaux MC, Jones CM, Adams D, Chetelat R, Bennett A, Powell A (2005) QTL analysis of fruit antioxidants in tomato using Lycopersicon pennellii introgression lines. Theor Appl Genet 111: 1396–1408

Rousseeuw PJ, Leroy AM (2003) Robust Regression and Outlier Detection. Wiley-VCH, Hoboken, NJ

Schauer N, Semel Y, Roessner U, Gur A, Balbo I, Carrari F, Pleban T, Perez-Melis A, Bruedigam C, Kopka J, et al (2006) Comprehensive metabolic profiling and phenotyping of interspecific introgression lines for tomato improvement. Nat Biotechnol 24: 447–454

Semel Y, Nissenbaum J, Menda N, Zinder M, Krieger U, Issman N, Pleban T, Lippman Z, Gur A, Zamir D (2006) Overdominant quantitative trait loci for yield and fitness in tomato. Proc Natl Acad Sci USA 103: 12981–12986

Serina L, Blondin C, Krin E, Sismeiro O, Danchin A, Sakamoto H, Gilles AM, Barzu O (1995) Escherichia coli UMP-kinase, a member of the aspartokinase family, is a hexamer regulated by guanine nucleotides and UTP. Biochemistry 34: 5066–5074

Slocombe SP, Schauvinhold I, McQuinn RP, Besser K, Welsby NA, Harper A, Aziz N, Li Y, Larson TR, Giovannoni J, et al (2008) Transcriptomic and reverse genetic analyses of branched-chain fatty acid and acyl sugar production in Solanum pennellii and Nicotiana benthamiana. Plant Physiol 148: 1830–1846

Sokal RR, Rohlf FJ (1995) Biometry: The Principles and Practice of Statistics in Biological Research, Ed 3. WH Freeman, New York

Stacklies W, Redestig H, Scholz M, Walther D, Selbig J (2007) pcaMethods: a Bioconductor package providing PCA methods for incomplete data. Bioinformatics 23: 1164–1167

Stitt M, Sonnewald U (1995) Regulation of metabolism in transgenic plants. Annu Rev Plant Physiol Plant Mol Biol 46: 341–368

Stitt M, Sulpice R, Keurentjes J (2010) Metabolic networks: how to identify key components in the regulation of metabolism and growth. Plant Physiol 152: 428–444

Studart-Guimarães C, Gibon Y, Frankel N, Wood CC, Zanor MI, Fernie AR, Carrari F (2005) Identification and characterisation of the alpha and beta subunits of succinyl CoA ligase of tomato. Plant Mol Biol 59: 781–791

Sulpice R, Tschoep H, Von Korff M, Bussis D, Usadel B, Hohne M, Witucka-Wall H, Altmann T, Stitt M, Gibon Y (2007) Description and applications of a rapid and sensitive non-radioactive microplate-based assay for maximum and initial activity of D-ribulose-1,5-bisphosphate carboxylase/oxygenase. Plant Cell Environ 30: 1163–1175

Tanksley SD, Ganal MW, Martin GB (1995) Chromosome landing: a paradigm for map-based gene cloning in plants with large genomes. Trends Genet 11: 63–68

Thevenot C, Simond-Cote E, Reyss A, Manicacci D, Trouverie J, Le Guilloux M, Ginhoux V, Sidicina F, Prioul JL (2005) QTLs for enzyme activities and soluble carbohydrates involved in starch accumulation during grain filling in maize. J Exp Bot 56: 945–958

Tieman D, Taylor M, Schauer N, Fernie AR, Hanson AD, Klee HJ (2006) Tomato aromatic amino acid decarboxylases participate in synthesis of the flavor volatiles 2-phenylethanol and 2-phenylacetaldehyde. Proc Natl Acad Sci USA 103: 8287–8292

Tikunov Y, Lommen A, de Vos CH, Verhoeven HA, Bino RJ, Hall RD, Bovy AG (2005) A novel approach for nontargeted data analysis for metabolomics: large-scale profiling of tomato fruit volatiles. Plant Physiol 139: 1125–1137

Till BJ, Colbert T, Codomo C, Enns L, Johnson J, Reynolds SH, Henikoff JG, Greene EA, Steine MN, Comai L, et al (2006) High-throughput TILLING for Arabidopsis. Methods Mol Biol 323: 127–135

Usadel B, Blasing OE, Gibon Y, Retzlaff K, Hohne M, Gunther M, Stitt M (2008) Global transcript levels respond to small changes of the carbon status during progressive exhaustion of carbohydrates in Arabidopsis rosettes. Plant Physiol 146: 1834–1861

Van der Hoeven R, Ronning C, Giovannoni J, Martin G, Tanksley S (2002)

Deductions about the number, organization, and evolution of genes in the tomato genome based on analysis of a large expressed sequence tag collection and selective genomic sequencing. Plant Cell **14:** 1441–1456

Villalta I, Bernet GP, Carbonell EA, Asins MJ (2007) Comparative QTL analysis of salinity tolerance in terms of fruit yield using two Solanum populations of F7 lines. Theor Appl Genet **114:** 1001–1017

Wang H, Schauer N, Usadel B, Frasse P, Zouine M, Hernould M, Latche A, Pech JC, Fernie AR, Bouzayen M (2009) Regulatory features underlying pollination-dependent and -independent tomato fruit set revealed by transcript and primary metabolite profiling. Plant Cell **21:** 1428–1452

Yelle S, Chetelat RT, Dorais M, Deverna JW, Bennett AB (1991) Sink metabolism in tomato fruit. 4. Genetic and biochemical analysis of sucrose accumulation. Plant Physiol **95:** 1026–1035

Yelle S, Hewitt JD, Robinson NL, Damon S, Bennett AB (1988) Sink metabolism in tomato fruit. 3. Analysis of carbohydrate assimilation in a wild species. Plant Physiol **87:** 737–740

Zamir D (2001) Improving plant breeding with exotic genetic libraries. Nat Rev Genet **2:** 983–989